THE GEOLOGY, GEOCHEMISTRY AND MINERALIZATION OF THE SOUTH WINDARRA, NICKEL ORE DEPOSIT, W.A.

by

J. SANTUL, B.Sc.

Submitted in partial fulfilment of the degree of B.Sc (Honours) in Geology at the University of Adelaide.

1975

CONTENTS

LIST OF FIGURES AND TABLES

ABSTRACT

A geochemical and mineralogical study has been carried out on the South Windarra Archaean nickel deposit, W.A. Within the ultramafic pile a series of flows has been identified. Two mineralized ultramafics form the base of this sequence, while thinner barren flows, with typical spinifex textures, overlie.

The two types of ultramafics are compared, with the intention of providing useful parameters for discriminating between barren and mineralized units. The comparison is made using data from field relationships, thin sections, polished sections together with geochemical analyses of whole rocks and trace elements (Ni, Cr, Zn, V, S).

It is concluded that sulphides were concentrated at depth, as an immiscible liquid in an ultramafic magma, prior to extrusion. This ultramafic magma consisted of abundant olivine crystals forming a crystal mush viscous enough to hold an immiscible sulphide fraction. Barren units have higher Ca and lower Mg and are considered to have been less viscous due to a lower crystal content and differing composition. These were unable to sustain an immiscible sulphide fraction.

INTRODUCTION

South Windarra (Poseidon, W.M.C. Joint Venture) lies 15 km south of the Mt. Windarra deposit, situated some 270 km NNE of Kalgoorlie, in the Mt. Margaret Goldfield of the Yilgarn Archaean Block, W.A. (See Fig. 1).

At South Windarra, nickel sulphides of economic grade were drilled in February 1971 by the consortium Union Oil Development Corp., Australian Hanna Ltd. and Homestake Iron Ore Co. of Australia Ltd. The Discovery was made beneath 30 m of alluvial overburden, following ground magnetometer surveys to locate the position of the potential Banded Iron Formation, ultramafic contact.

Previous work on the area has been essentially confined to Mt. Windarra. Geochemical and structural theses have been carried out by Davidson, Watchman, Drew, Leahey and Drake while reports have been written by Roberts and Robinson, Stock and Wright. Petrological and mineragraphic reports have also been compiled on Sth. Windarra by A. Whittle and Associates, W. Fander and A.M.D.E.L.

The aim of the project was:

(1) to define a stratigraphy in the ultramafic pile as exposed in the open pit.

(2) to provide parameters such as geochemistry, mineralogy and textures for distinguishing ore bearing ultramafics from barren ultramafics, as useful features for nickel exploration.

(3) to determine the geochemistry of the ore body and surrounding envelope, including both conformable and transgressive elements.

Over/

The work done included:

(a) mapping and detailed logging of drill core in two periods, December 1974 - February 1975 and August 1975.

(b) study of approximately 150 thin sections and 42 polished sections.

(c) 120 whole rock analyses

(d) Ni, V, Cr, Zn for 325 samples, and S for 85 samples.

All samples described should be preceded by the number 451. This represents the accession number given to the author by the University of Adelaide.

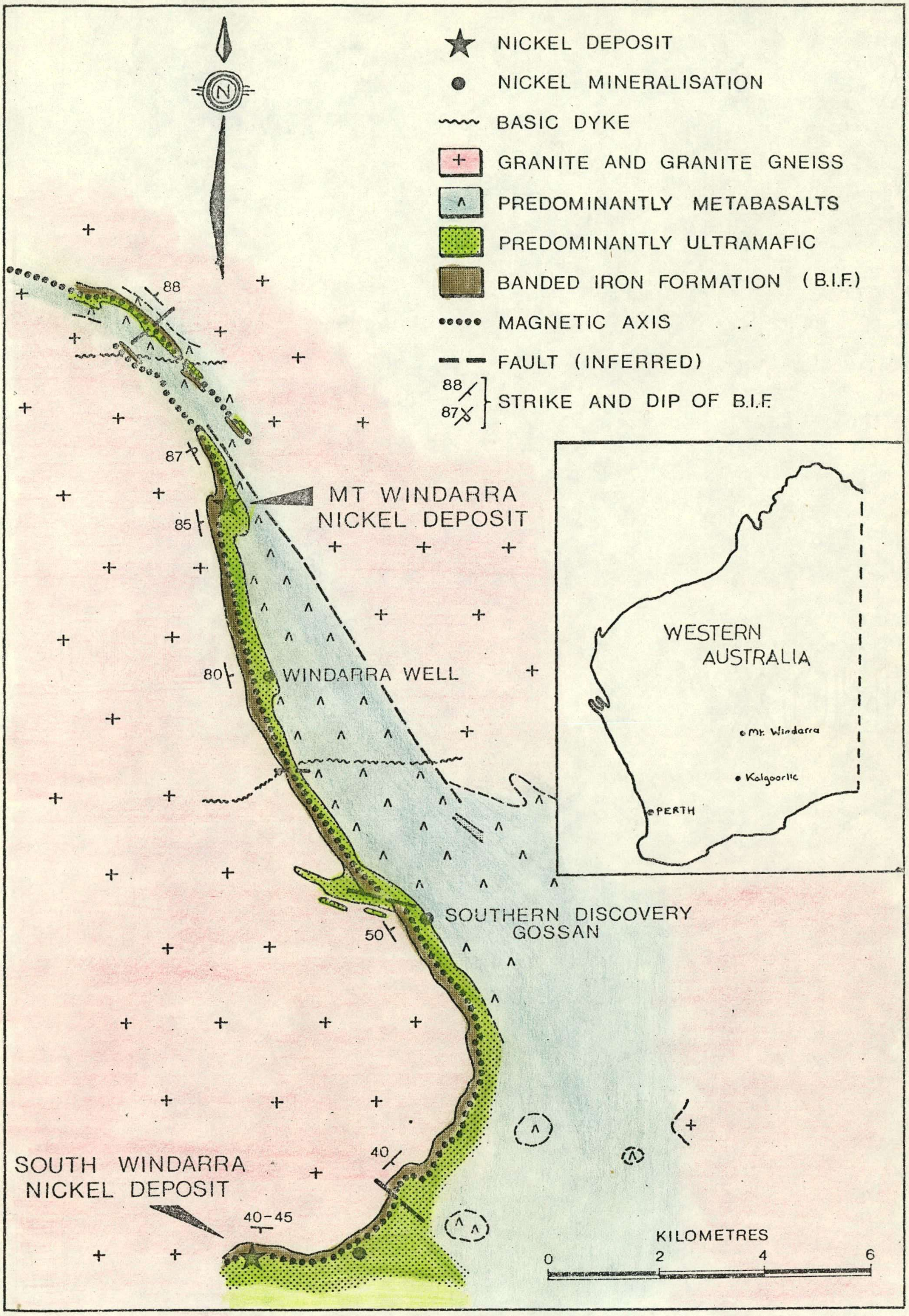

Fig. 1. Location map (after Poseidon Limited)

GENERAL GEOLOGY

The Windarra region is part of the Mt. Margaret Goldfield, where granite gneisses enclose N to NW trending belts of metavolcanics, metasediments and intrusive rocks, termed greenstone belts. Nickel mineralization is found at the base of the Archaean ultramafic rocks of the greenstone belt, similar to other areas such as Kambalda, Scotia, Nepean and Redross.

The ore zone of Sth. Windarra occurs on the northern margin of an E - W trending ultramafic sequence of serpentinites and tremolite/chlorite schists in contact with a Banded Iron Formation (B.I.F.). The BIF is bordered to the north by an intrusive gneissic granite, while the ultramafics are overlain conformably by a thick sequence of high Mg metabasalts (See Fig. 1). Further south, granites enclose the greenstone belt. This greenstone sequence dips south at 40 - 45°, compared with the steeply dipping Mt. Windarra sequence (see Fig. 5).

Felsic-mafic intrusives transgress all elements of the stratigraphy and include feldspar porphyry dykes, dolerite dykes and a "transgressive ultramafic" (mine terminology). Intrusions are orientated generally either N - S or NW - SE (see Fig. 3).

The ultramafic sequence consists of multiple extrusive lavas based on the evidence of spinifex zones, geochemistry and breccias. Two mineralized ultramafic units (up to 60 m thick) have been defined by this study and consist of dominantly serpentine with a basal concentration of nickel ore. These occur at the base of the ultramafic pile. Thinner flows with typical spinifex textures, as described by Nesbitt (1971) exist either between the mineralized flows or more commonly overlying. These are barren in sulphides. From the asymmetry of spinifex textures the sequence is facing south.

The majority of the ore occurs at the base of the ultramafic sequence and consists of two main lenses up to 230 m long and 25 m wide. Remaining mineralization forms in sulphide concentrations in a higher ultramafic flow and is termed hanging wall mineralization. In general the ore zone consists of a massive ore, dominant in the west, overlain by a thicker disseminated zone. It comprises of pyrrhotite, pentlandite (invariably altered to violarite), pyrite with basal concentrations of both chromite and pyrite.

Original igneous rocks have experienced metamorphism plus alteration by processes of serpentinization, talc-carbonate alteration and K-metasomatism.

Significant folding and faulting controls the distribution of the ore zones. Domings in the BIF result in shear and fault development, forming embayments in the ultramafics.

Compared to Mt. Windarra, Sth. Windarra is associated with the same sequence of rock types but differs in that intrusions are more numerous, the BIF has less Fe (see Table 1) and there exists no jaspilite ore whereby Ni concentrates in economic values in the BIF (Leahey, 1973).

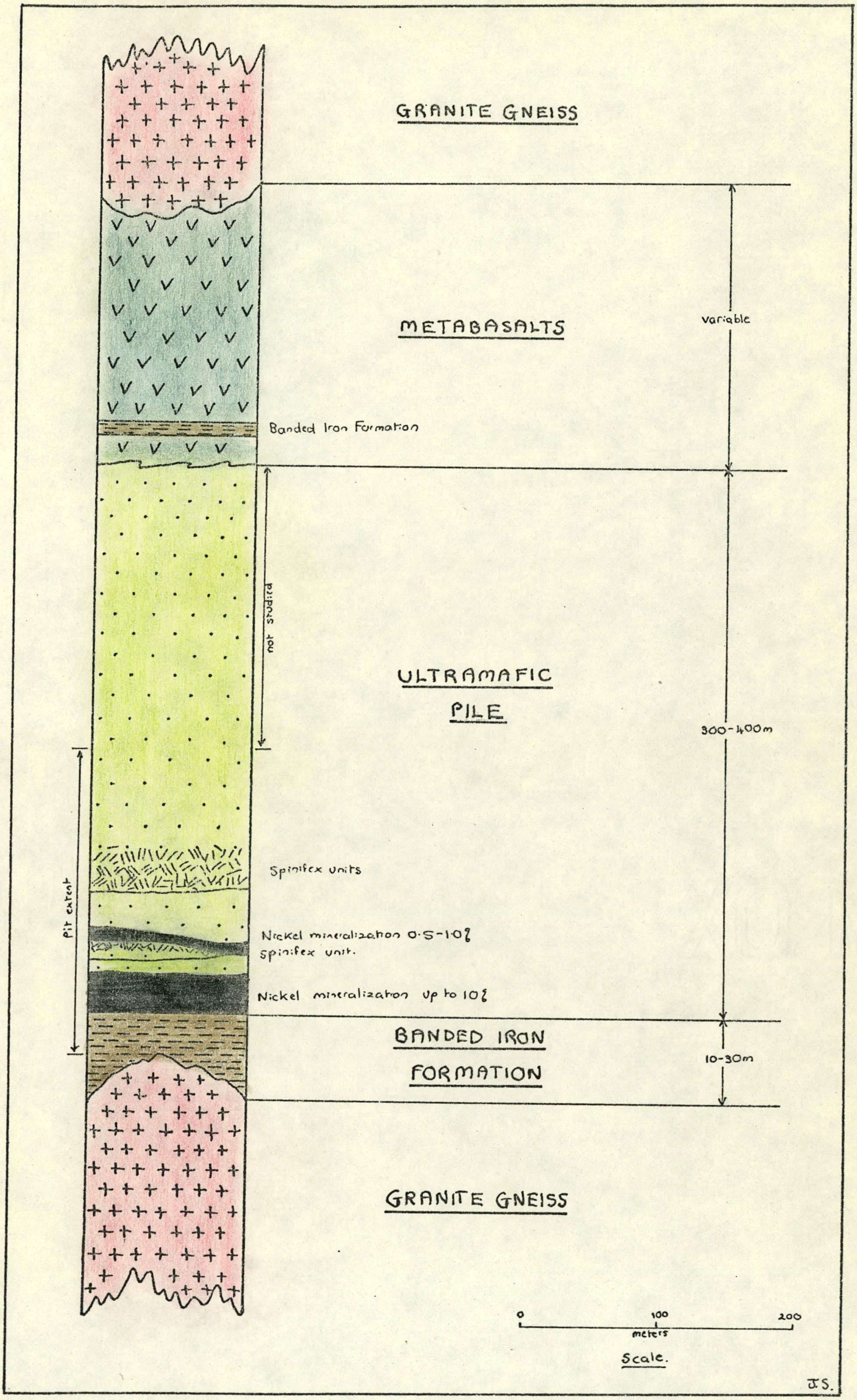

Fig. 2 Stratigraphy of the greenstone belt of Sth. Windarra

LEVEL PLAN RL10360

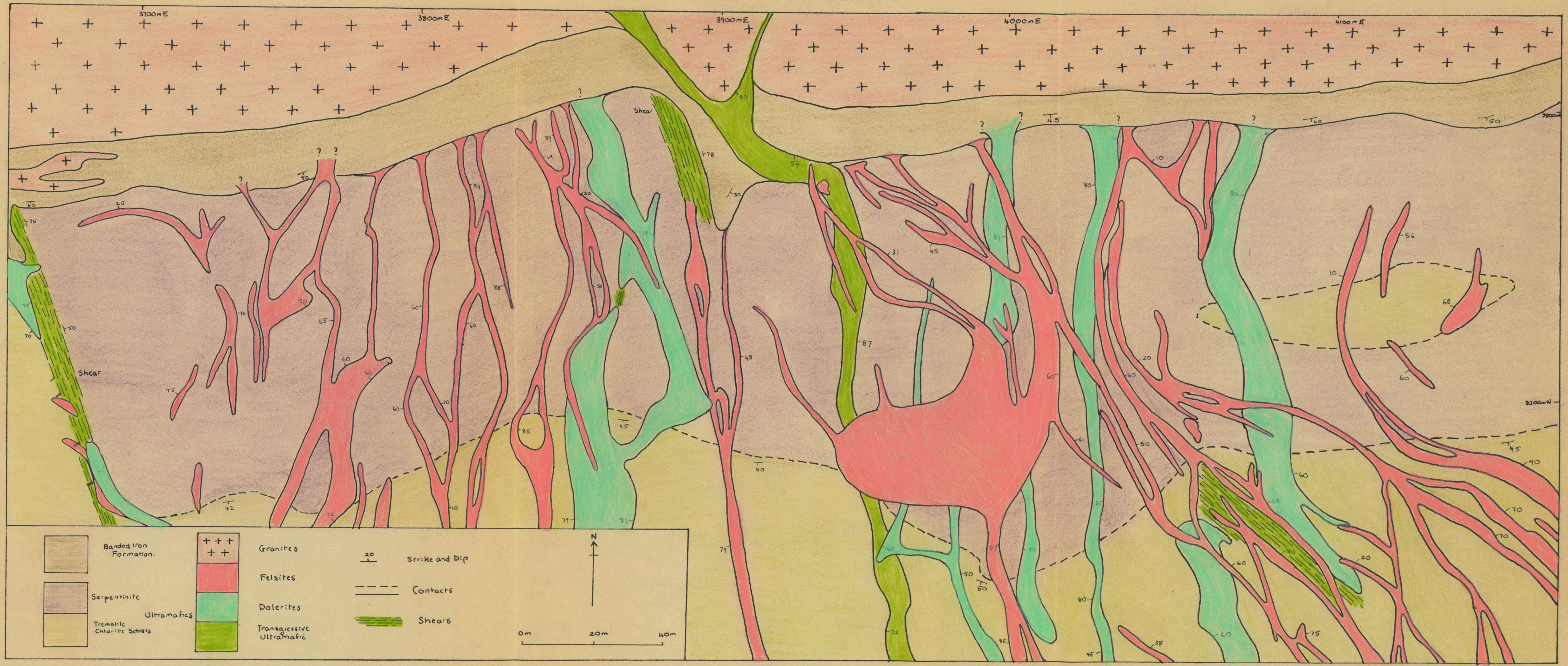

FIG.3 Level Plan RL10360 of Interpreted Factual Mapping (after J.L., D.C., J.S.)

PETROLOGY

Banded Iron Formation

Geochemically these rocks are ferruginous cherts with alternating layers of SiO_2 and Fe rich minerals, varying from a few mm to several cms. Mineralogically they consist of a great variety of rock types, divisible into metamorphosed pure and impure carbonate and sulphide facies (Drake 1972) with minor intercalated pelitic horizons.

The major minerals present are quartz, amphibole, biotite and magnetite together with minor carbonate, garnet, apatite and sphene. Main assemblages include (see Appendix A).

- (a) quartz - cummingtonite/grunerite - magnetite
- (b) quartz - cummingtonite/grunerite - hornblende-magnetite
- (c) quartz - biotite - magnetite
- (d) quartz - actinolite - magnetite
- (e) quartz - biotite - garnet (almandine by X.R.D.) How?

These assemblages place metamorphic grade within the amphibolite facies (Groves et al, 1974,5).

The BIF macroscopically is banded, with the banding parallel to the ore contact. In general the more Ca, K rich varieties occur closer to the contact of the ultramafic and BIF, with intercalations of pelitic horizons throughout. Similarly sulphide rich types exist near the contact.

Contact Zone

Ultramafic/metasediment contact rocks are considered to be the sheared equivalent of Jahns (1967) metamorphic differentation sequence. In general contact rocks are variable, however the most common assemblages found are (as in Appendix A):

Contact Zone (Continued)

BIF:	Amphibole/quartz/magnetite	
Blackwall Contact Zone:	(	Chlorite/phlogopite
	(	Breccia with Ab porphyry aggregates and garnet.
	(	Tremolite/talc-carbonate
Ultramafic:	Serpentine/talc-carbonate	

The presence of phlogopite, talc and albite imply that element migration between ultramafic and highly siliceous country rock has taken place. This can be equated with the blackwall zones of other bodies as described by Jahns (1971) and Stolz (1971) whereby migration of Si, Na, K into the ultramafic and Fe, Mg out have occurred.

Some steatitization (Hess, 1933) exists, however normally talc is intergrown with carbonate suggesting talc-carbonate alteration is extensive along the contact. Being a zone of weakness the contact has acted as a channelway for CO_2 rich solutions. This is supported by the fact that talc-carbonate alteration decreases away from the contact.

Ultramafics:

The ultramafics are devoid of any primary mineralogy due to the extensive metamorphism, but original textures are still preserved. However a large variety of rock types exist ranging from serpentinites, talc-carbonate assemblages, chloritic schists to tremolite/chlorite assemblages.

From both geochemical and petrographical data the ultramafics can be subdivided into several lithological units (see Fig. 4). These are as follows, from south to north:

(1) numerous thin spinifex topped units ranging from 5 m to 25 m in thickness.

(2) thick hanging wall mineralized ultramafic (HWMU) of massive serpentinite (40 m).

(3) barren thin spinifex topped lens (10 m).

(4) main ore bearing ultramafic of serpentinite (40 m).

(a) Main Ore Bearing Unit:

Thicknesses vary from 25 m in the east to 45 m in the west, where Ni mineralization is greatest (see 'Mineralization'). The limit of the unit is defined by a chlorite/magnetite schist (061, Appendix A) with a talc/chlorite breccia above, or by a weak chlorite/tremolite breccia at the base of the barren thin spinifex lens between the two mineralized units.

The composition of the ore bearing unit is quite homogenous with serpentine making up the bulk of the body. Serpentinization of olivine has been complete, resulting in some primary textures being outlined by magnetic trails (Fe expelled by serpentinization, Watchman, 1971).

Lamellae serpentine (antigorite by XRD) pseudomorphs are coarse grained, equant and close packed in the centre of the body (see Fig. 5) but towards the margins these become more elongate and sit in a fine matrix of feathery serpentine and flaky chlorite, representing a more Al rich liquid expected at margins of flows (Wilson et al 1969, see Fig. 6).

A significant aspect of some serpentinites here is that often primary textures are destroyed by the metamorphism, whereby antigorite is dehydrated to produce coarse elongate olivine grains (Evans and Trommsdorf, 1974; Groves et al 1975). This metamorphic olivine has been altered back to serpentine, leaving a "triangular texture" with opaques infilling laths.

Talc-carbonate alteration is ubiguitous throughout the unit with two periods evident.

(1) after the first serpentinization (here later serpentine replaces carbonate).

(2 after the main metamorphism and preceding the second serpentinization.

Carbonate (magnesite, dolomite by X.R.D.) often replaces along serpentine boundaries or on lamellae and in general is greatest near the metasediment/ore zone contact.

(b) Barren thin Spinifex Unit (between mineralized units):

This unit reaches up to 10 m in thicknesses and lies between the two mineralized serpentine rich ultramafics in the east (see Fig. 4). Along strike and down dip it lenses out. It is defined by a chloritic schist (226, Appendix A) and breccia at the base and sometimes by a talc/chlorite schist overlying random spinifex at the top. Spinifex textures as described by Nesbitt (1971) are invariably found (see Fig. 6).

Mineralogically it contains at the base; serpentine, tremolite, talc-carbonate, chlorite and opaques grading into a strong tremolitic/chloritic schist with relict spinifex (see Appendix A). All the features of a typical spinifex ultramafic unit are found (Fig. 6) i.e. a massive serpentine rich zone, overlain by a skeletal zone of platey spinifex and then random spinifex.

The presence of tremolite, chlorite and spinifex textures confirm that the unit is of a pyroxenite peridotite parentage. The fact that it is of a different composition from the ore bearing unit and that it is barren is significant (see 'Discussion').

(c) Hanging Wall Mineralized Unit:

Thicknesses vary from 35 - 55 mm with the unit thickest in the west. Here it is in direct contact with the main ore bearing unit. To the east the unit thins and overlies the barren spinifex unit above.

Mineralogically it is similar to the ore bearing unit and consists of serpentine, minor talc-carbonate and chlorite. Again chlorite concentrates to the margins. Texturally the centre has equant serpentine megacrysts giving way above and below to megacrysts in a more extensive fine matrix of serpentine/chlorite. Sulphides concentrate at the base as disseminations.

Talc-carbonate alteration is abundant where felsites intrude the ultramafic (WSD 93, Appendix A) Naldrett (1967) relates talc-carbonate alteration to CO_2 rich solutions from granitic sources.

The upper limit of the unit is defined by a chloritic breccia or by a change in mineralogy with the introduction of tremolite. No spinifex zones exist.

(d) Thin Spinifex Units:

Overlying the two mineralized ultramafics, several thin units with spinifex tops occur, varying in thickness from 5 m to 25 m. Individual units are recognised by the presence of chilled contacts, breccias, distribution of textures and marked compositional changes and trends. Many textures are identical to those primary igneous textures found by Nesbitt (1971), Pyke et al (1972), even though alteration is extensive. They are typical in that subdivision is possible into; massive dunite unit, porphyritic zone, plate spinifex, random spinifex and breccia (see Fig. 6).

Mineralogically units consist of tremolite, chlorite, magnetite schists with occasional serpentine/tremolite/ chlorite basal zones. The tremolite, chlorite spinifex zone is restricted to the upper half. Most unit interfaces show a strong breccia zone of rounded tremolite/chlorite fragments in a finer matrix of chlorite and talc.

(e) Chloritic Schists:

Several horizons of dark green chlorite schists occur within the ultramafic. Their origin is either

(1) shear zones

(2) contact metamorphic selvages of nearby intrusions.

(3) chemical sumps where Mg, Fe, Si concentrate from serpentinization ((Williams, 1971); 192 Appendix A).

These are not to be confused with the chlorite talc breccias found between units although similarities exist. Breccias can be traced laterally compared with the above schists.

(f) Petrological Conclusions

A distinct compositional variation exists between the thick mineralized ultramafics and thinner barren spinifex types.

Mineralized units consist chiefly of serpentine megacysts in a matrix of fine serpentine and sometimes chlorite. They have no spinifex zones at the top and are believed to represent a dunitic parentage.

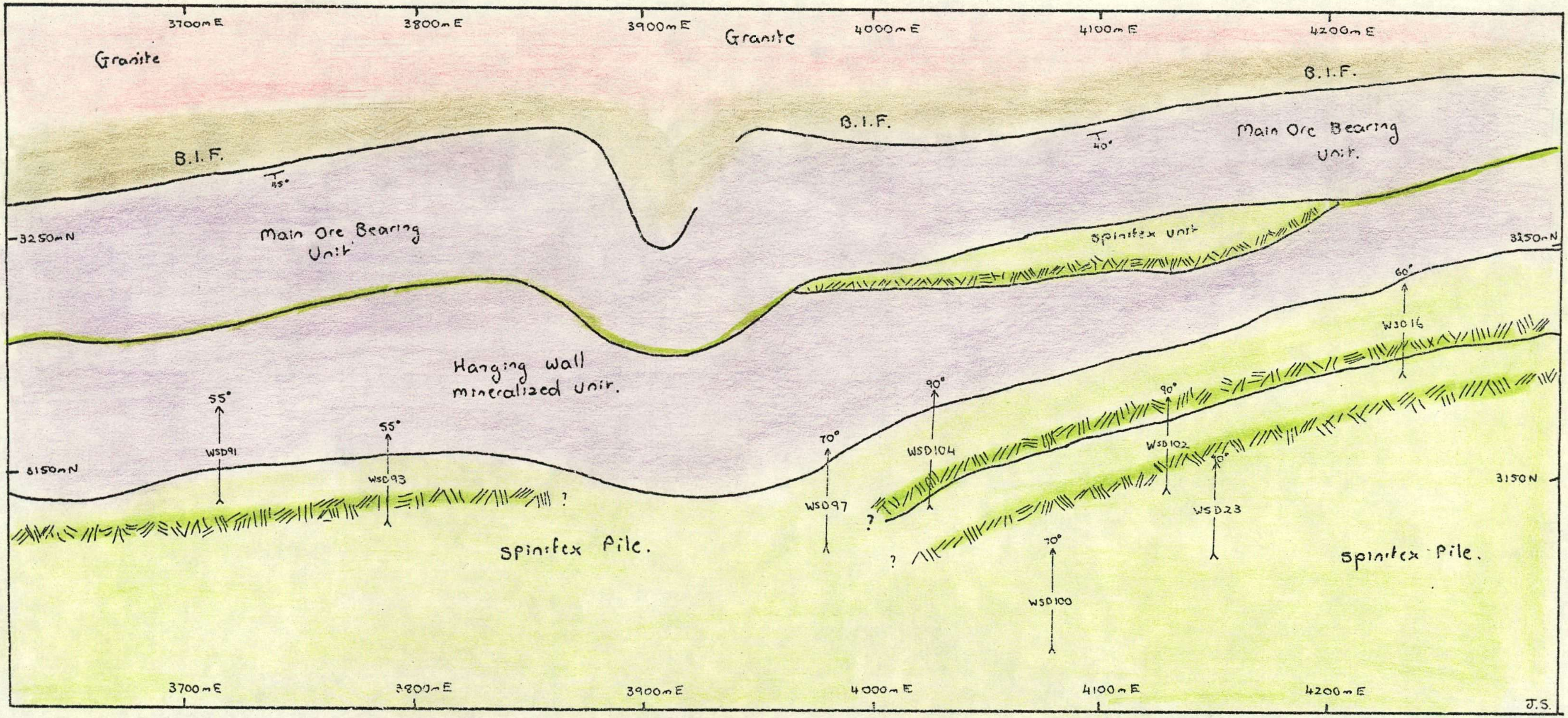

Fig. 4 Level plan (RL 10 360) of (a) interpreted ultramafic flows as by surface mapping and drill hole correlation.
(b) location of diamond drill holes used in this study (angle of hole shown at top of arrows).

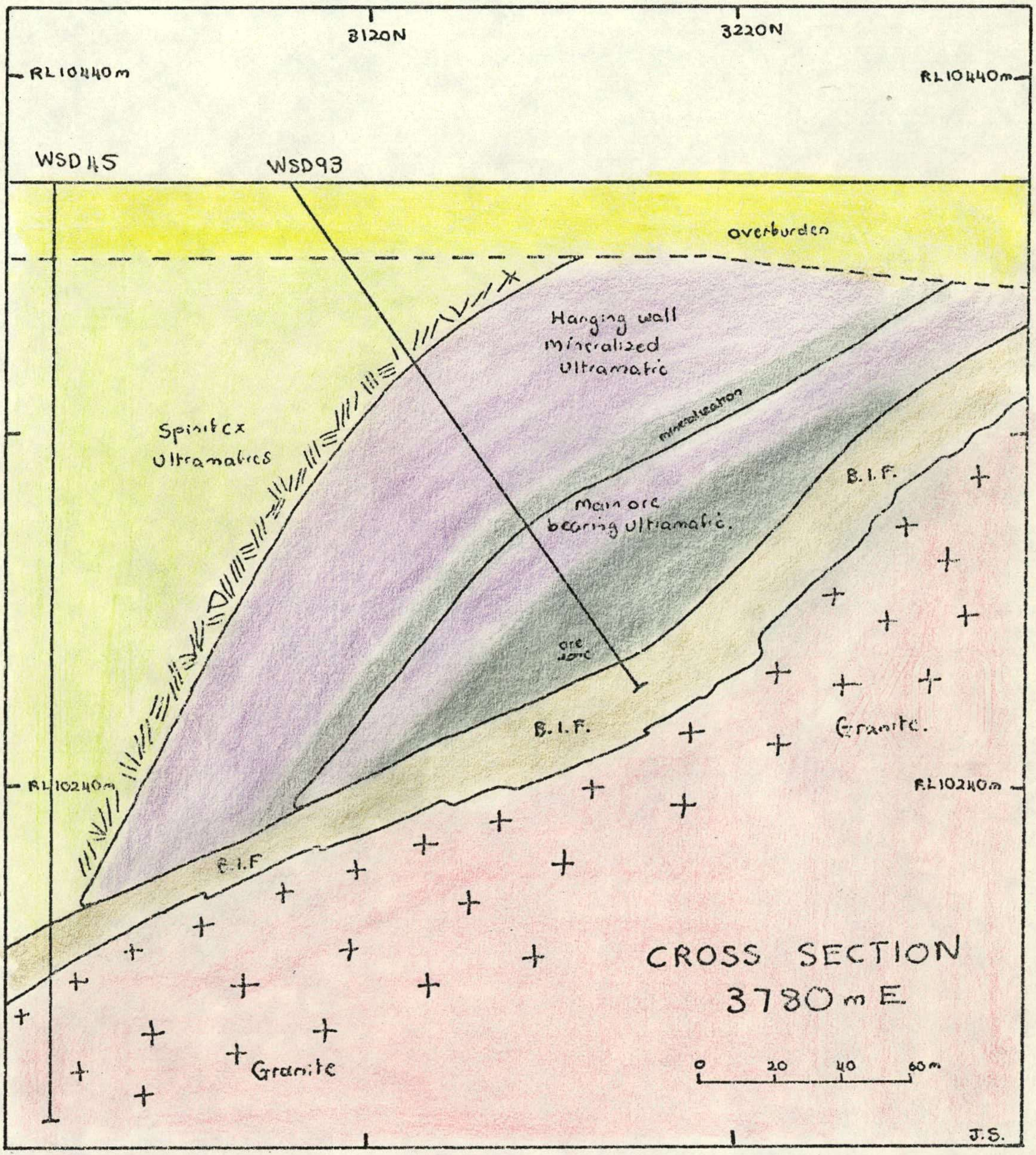

Fig. 5 Cross section through ultramafics showing lensoidal shape of mineralized ultramafics.

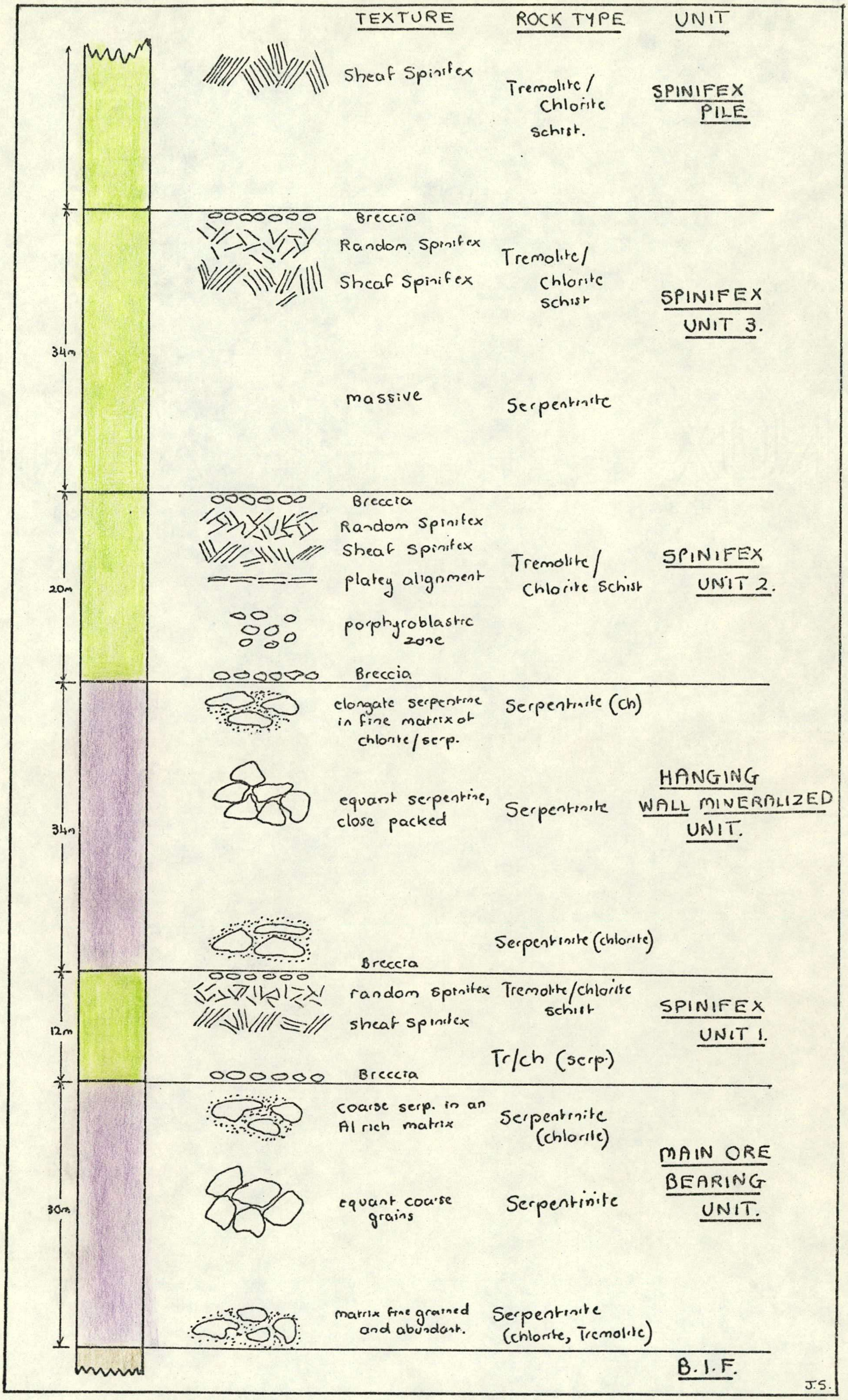

Fig. 6 Petrography and textures found in DDH WSD 100

Barren units are distinguished by the presence of tremolite, chlorite and very little serpentine. Spinifex zones and breccias are common. These features suggest they were extruded as pyroxenitic peridotites.

Metabasalts:

Macroscopically metabasalts are recognised by their massive, dark green appearance with occasional breccia horizons and layering. In thin section they consist of amphibole (both hornblende and actinolite), quartz, plagioclase, sphene, epidote, and minor biotite, opaques and apatite (see Appendix A). Alignment of minerals is common. K and Ca (biotite and epidote) metasomatism has been extensive in some cases and thus places reservations on geochemical interpretations.

Whole rock analyses (Table 2) indicate they are high Mg basalts similar to other metabasalts of the Eastern Goldfields, except here alteration is more extensive.

Intersected in deeper drill holes was a BIF horizon in the metabasalts, near the base of the sequence. Thickness of this unit is about 3 m. It consists of mainly hornblende, biotite, magnetite and quartz together with minor plagioclase and apatite (482, Appendix A). Banding is present.

Dolerites:

Intrusive dykes of a mafic composition cut the ultramafic, metabasalts and BIF in a N - S direction. Most are near vertical and commonly reach 10 m in width. These metamorphosed dolerites consist of: amphibole (hornblende or actinolite) 65%, quartz 20%, plagioclase 10%, opaques 5% with accessory apatite, epidote, zircon, sphene and carbonate. Macroscopically they are green, fine to coarse-grained amphibolites, weathering to a distinctive yellow colour.

Commonly foliated margins exist with chlorite/magnetite schists representing contact metamorphism.

Dolerites were intruded early in the history of the intrusive elements of the area and often show subsequent shearing or intrusion by felsites, (see Fig. 3). At least two periods of intrusion took place with minor thin varieties coming last.

Granites:

Granitoid rocks occur north and south of the greenstone belt, both below the BIF and south of the metabasalts.

The northern granite is a strongly foliated quartz-microcline-albite-biotite granite gneiss with minor muscovite, chlorite, carbonate and apatite. Compositionally it is a granodiorite with the main plagioclase being oligoclase or albite. Intense lineation structures of biotite are most evident near the contact of the BIF and granite. Retrograde alteration of biotite to chlorite is common and related to the last hydration of the greenstone.

Macroscopically the southern granite is similar.

Within the ultramafic pile in the west of the pit area, a muscovite rich granodiorite exists. The relationship of it to other granites is obscure due to lack of outcrop and drill hole data, however the complex folding and shearing appear to be of significance.

Feldspar Porphyry Dykes

Numerous metamorphosed felsitic porphyry dykes and lenses intrude all lithologies. These occur either N - S orientated or if intruded along major shears NW - SE. At least four periods of intrusion exist ranging from those before dolerites, after dolerites, along shears and after the intrusion of the "transgressive ultramafic".

The typical mineralogy comprises plagioclase phenocrysts set in fine quartz-feldspar, biotite groundmass with the main feldspar being predominantly albite (see Plates). Accessories include chlorite, apatite, minor sulphides, epidote, zircon, muscovite, sphene and talc-carbonate. Sericitization of plagioclase is common.

Several varieties can be seen based on colour, grain size and composition however no relationship of type and age of intrusion was found.

All felsites are metamorphosed, some more recrystallized than others, but relict igneous textures including plagioclase zoning can still be seen. Retrogression has also taken place.

Contact metamorphism is evident where felsites intrude the ultramafic. Here biotite, chlorite and talc form thin selvages up to 10 cms wide around intrusions. In thin section contact metamorphism is shown by the mobility of elements from the intrusion. The least mobile is Ca^{++} (epidote) to K^{+} (biotite) to Al^{3+} (chlorite) to the most mobile Si^{4+} (talc).

Similarly talc-carbonate alteration can be related to these acid intrusions.

"Transgressive Ultramafic"

In outcrop the "transgressive ultramafic" runs approximately N - S transecting the BIF (see Fig. 3). It has a variable thickness of 10 - 20 m and is often steeply dipping. Shearing is common within the body but it is thought that the body intruded along a major shear zone late in the magmatic history.

Macroscopically it consists of a strong biotite schistosity throughout a more massive dark green amphibole rich rock. Mineralogically the "transgressive ultramafic" is quite variable, comprising predominantly of amphibole (hornblende, tremolite, or actinolite), biotite, quartz and feldspar, chlorite, opaques and minor accessory sphene, apatite and zircon. Talc-carbonate alteration is common near the margins.

Typical composition is; amphibole 40%, quartz and feldspar 15%, chlorite 25%, biotite 25%, opaques 5%.

Whole rock analyses (see Geochemistry) suggest the body is highly differentiated and similar to spinifex ultramafics, except with less MgO and more Al_2O_3.

Metamorphism:

Both prograde and retrograde metamorphism is evident. Hydration of the greenstone sequence took place soon after extrusion, resulting in serpentinization of the ultramafic sequence. Amphibolite metamorphism preceded, in the formation of metamorphic olivine, related "triangular texture" and recrystallization. The stability of muscovite, presence of almandine, blue-green hornblende in basics indicates the grade is lower to middle amphibolite.

This metamorphism has affected most elements of the greenstone belt and is related to the major deformation of the belt (Drake, 1972).

Hydration followed resulting in complete serpentinization of the ultramafic sequence. Retrogression in other rocks related to this is common.

MINERALIZATION

Nickel mineralization occurs over an E - W strike length of 1,280 m and dips 40 - 45°S. Ore occurs in two main lenses individually about 230 m in length and varying up to 25 m in width. The bulk of the current ore mined is in contact with the underlying BIF and represents contact mineralization.

Hanging wall mineralization exists at the base of a second serpentine rich ultramafic flow, 40 - 50 m above the contact mineralization, but due to the small thickness and low grade it does not enter into ore reserve calculations and is insignificant in mining.

Primary mineralization includes;

(1) Massive ore
(2) disseminated ore
(3) breccia ore.

No jaspillite ore (Leahey, 1973, Mt. Windarra), where Ni concentrates in economic values in the BIF adjacent to the massive ore, exists. This is most likely a reflection of the lower pyrite, pyrrhotite content of the BIF whereby Ni diffusion can be uptaken (Ewers, 1971).

Main Ore-bearing Unit:

(a) Massive Ore

Massive ore is evident in the west of the pit where the main ore bearing ultramafics are thickest. Here sulphides usually reach up to 80% with the average mineralogy being: Violarite (plus relict pentlandite) 35%, pyrite 30%, pyrrhotite 25%, magnetite 10% with minor chalcopyrite.

Magnetite often has chromite cores in larger individual grains but usually forms as veinlets as found at Scotia (Stolz, 1971).

The ore comprises of coarse allotriomorphic granular textured violarite and pyrrhotite amongst large porphyroblasts of pyrite, indicating intense recrystallization and annealing. In general the grain size of ore components is greater than other ores, with pyrrhotite and violarite up to 0.2 mm and pyrite up to 1 cm.

Little folding and buckling of thin silicate strands within pyrrhotite and violarite has been found in the massive ore, even though this exists in the disseminated ores (see Appendix B).

Most exposures of the base of the massive ore show a diffuse contact into the BIF represented by a breccia ore. Here concentration of equant rounded grains of chromite up to 0.5 mm exists, similar to that described by Ewers and Hudson (1972) at Kambalda, (See 'Discussion').

Within and above the massive ore a pyrite rich zone is noticeable, consisting of coarse porphyroblasts of pyrite up to 2 cm sitting in a finer matrix of pyrrhotite and violarite (097A, Appendix B).

Chalcopyrite is less common than in the Mt. Windarra massive ores, but when present it is fine grained and in common association with pyrite porphyrobasts.

(b) Breccia Ore:

Fragments of albite-quartz porphyroblastic schists, quartz, tremolite/chlorite or actinolite/chlorite schists sit in a sulphide rich matrix. These fragments (60% of the breccia) often reach up to 4 cm in length and are equated with Jahns (1967) metamorphic differentiation zone between ultramafics and country rocks. The presence of almandine garnet and gnarled appearance of gangue fragments implies that this reaction zone has been highly deformed at high temperatures. Such deformation is expected in massive sulphides occuring on a contact between rock types of vastly different competance.

The sulphide assemblage consists dominantly of pyrite, pyrrhotite, violarite plus pentlandite and minor chalcopyrite. Pyrrhotite occurs as tightly welded aggregates with violarite forming the matrix for coarser grained (up to 0.5 mm) pyrite subhedra. Evident in the field pyrite porphyroblasts show prominant banding parallel to the layering in the BIF.

Violarite shows often relict pentlandite and if fine grained (0.15 mm) interlocking with aggregates of pyrrhotite. Adjacent pyrrhotite shows both exsolution flames of violarite and alteration to violarite around grain boundaries (see Plates).

(c) <u>Disseminated Ore</u>:

Disseminated sulphide ore (of ore grade > 0.8% Ni) generally reach 20 m in width, while disseminated sulphides occupy all of the ultramafic. Varying proportions of pyrrhotite, pentlandite plus violarite, pyrite and chalcopyrite are present in a host of dominantly serpentine-talc/carbonate rocks. Average composition is pentlandite/violarite 30%, pyrite 5%, pyrrhotite 35%, magnetite 30%.

Here sulphides either occupy laths formed by interlocking grains or surround coarser serpentine megacrysts. This nature implies the term "matrix sulphides" as preferred by Hancock et al (1971) is not applicable.

The main nickel mineral present is violarite with relict pentlandite (see Plates) however deeper holes show very little violarite with more pentlandite (WSD 100, Appendix B). The average Ni mineral content is about 30 - 35%*, increasing to the base to 55%. Both violarite and pentlandite exist as fine grained anhedra but grade up to form aggregates of interlayered strands with silicates (see Plates). This texture has been noted at Scotia (Stolz, 1971) and is thought to represent closeness to contacts. The ubiquitous nature here suggests it is a feature of the higher grade metamorphism and deformation existing.

Pyrrhotite similarly forms strands, but gives way to pyrite in the western part of the ultramafic (see note under HWMU).

Chalcopyrite and millerite are minor with chalcopyrite associated as medium grained elongate grains with pyrite. Millerite is erratic but when found exists as intergrowths with strands of pyrrhotite.

Magnetite contents vary (depends on the amount of carbonage alteration) from 20% to 70%. Most commonly it occurs as fine disseminations forming trails outlining serpentine. These are by-products of the serpentinization (Coleman, 1971).

* represent a percentage of the total opaque content.

Hanging Wall Mineralized Unit:

Mineralization is dominantly disseminated sulphides with no massive ore. Grades reach up to 1% Ni.

Sulphide contents are less than 15% of the total rock and consist of pyrrhotite, pentlandite (violarite in shallower holes) and pyrite. As with the disseminated sulphides of the main ore bearing body, the sulphides form around silicate grains generally interlayered as strands with fine silicates.

Average composition is:

in the west (WSD 93), pentlandite/violarite 20%
magnetite 40%, pyrite 40%.

in the east (WSD100), pentlandite/violarite 20%
magnetite 40%, pyrrhotite 30%
pyrite 10%.

The presence of pyrite over pyrrhotite in the western part of flow is contributed to the more extensive talc-carbonate alteration existing (see Appendix A, WSD 93). Eckstrand (1975), suggests this alteration is related to a high fugacity of sulphur hence pyrite forms, not pyrrhotite.

Barren Spinifex Ultramafics:

Those units with spinifex tops have little or no mineralization associated. Sulphides and magnetite form some 5% of the section with magnetite $>60\%$ of the opaque content.

One exception is the thin unit between the mineralized ultramafics where opaques reach 15% but Ni content is still low 2,000 ppm (see Appendix D). Those sulphides present are pyrite and pyrrhotite.

ORE GENESIS

The stratiform geometry of the ore and the fact that disseminated zones overlie massive ores at the base of the main ore bearing ultramafic, implies the magmatic segregation model is applicable. Since it has been shown that the ultramafic unit of the greenstone is a pile of thin units with the mineralized units reaching 50 m, insufficient S could be dissolved in the magma to form a high grade Ni deposit (Maclean, 1969, Skinner & Peck, 1969). Hence the sulphides present in both mineralized units must have been emplaced as immiscible Fe sulphide liquids in an ultramafic magma. The presence of a chromite rich base suggests this liquid was high in O_2 content.

There is no evidence of formation of the main sulphide body by sulphurization from the adjacent BIF since:

(1) the BIF contains very little sulphides, not enough to supply the S required.

(2) no Ni or Fe depletion zones in the mineralized ultramafics exists.

(3) the ultramafic flows are not thick enough to release large amounts of Ni on serpentinization for an ore deposit.

However definite upgrading of the deposit by some diffusion of Fe, S into the ultramafic has occurred.

The relationship of sulphide accumulation to composition of the ultramafic is an important one. Mineralization is only found in the serpentine rich, non spinifex topped ultramafics. The higher Ca, lower Mg spinifex units are barren. (See 'Discussion').

GEOCHEMISTRY

Samples were analysed for Ni, Zn, V, Cr by X-Ray fluorescence spectrometry (X.R.F.). Sulphur was determined by automatic titration methods, (see Appendix D).

Whole rock analses, also by the X.R.F., were carried out on 120 samples representing most rock types.

Banded Iron Formation

Five analyses of a range of compositionally different BIF's were done (see Table 1). Of note is the high SiO_2 content (65 - 80%) and lower Fe_2O_3 ($< 25\%$) than the common banded iron formation as stated by Gross (1965) in Table 1. Hence these are not true BIF's but should be called ferruginous cherts based on the SiO_2 content.

One sample (B100) is representative of a typical garnet, biotite schist horizon in the BIF. This rock is very rich in Fe, Al and higher in Ca, Mg, Mn, Ti and K than the more cherty BIF's. It is thought to represent an impure ferruginous pelitic horizon deposited amongst the chemically precipitated BIF (Drake, 1972).

On comparing whole rock analyses and petrology the Ca (reflection of actinolite) and K(biotite) content is highest near the ultramafic/metasediment contact as found by Drake (1972) at Mt. Windarra.

Considering trace element data two features are evident;

(1) Ni is highest closer to the ultramafic contact (up to 1,994 ppm, Table 1) implying Ni diffusion from the nearby massive ores has taken place.

TABLE I

Banded Iron Formation, Whole Rock Analyses

	303	309	464	473	Gross (1965)	B100
SiO_2	84.919	74.171	65.866	80.090	48.50	42.802
Al_2O_3	1.015	0.721	0.215	0.066	1.00	15.200
Fe_2O_3	8.815	18.994	25.334	17.045	42.10	28.949
MnO	0.612	0.660	0.600	0.620	0.00	1.740
MgO	1.145	2.194	4.382	1.620	2.20	6.011
CaO	1.690	1.921	2.554	1.519	1.20	4.446
K_2O	0.642	0.194	0.035	0.019	-	1.105
TiO_2	0.137	0.009	0.007	0.003	0.00	0.279
P_2O_5	0.060	0.130	0.033	0.051	-	0.072
Total	99.035	98.994	99.027	101.033	98.9	100.602
Loss	4.250	0.880	0.730	0.170	3.00	4.450
			Trace elements (ppm)			
Ni	1994	36	1544	22	-	108
Zn	4300	470	352	383	-	201
Cr	1	6	2	3	-	6
V	18	15	8	3	-	43

303: quartz-biotite-magnetite-carbonate

309: quartz-cummingtonite/grunerite-hornblende-magnetite

464: quartz - actinolite-magnetite

473: quartz-cummingtonite/grunerite-magnetite

B100: quartz-biotite-garnet-magnetite

Gross (1965): Oxide facies B.I.F.

TABLE 2

Analyses of Metabasalts and Dolerites

	474	478	40264 (Leahey)	63287 (Hallberg)	P1 (Viljoen)	135D	146D
SiO_2	50.020	41.753	52.94	53.01	51.06	47.989	50.056
Al_2O_3	7.347	8.118	10.28	12.76	8.71	13.792	13.327
Fe_2O_3	13.142	17.826	12.43	9.81	10.91	19.515	15.542
MnO	0.215	0.257	0.10	0.18	0.26	0.332	0.355
MgO	12.255	12.512	12.02	11.94	10.70	6.856	5.923
CaO	13.396	11.681	8.33	8.41	11.49	6.036	8.928
Na_2O	1.310	0.960	2.75	2.50	0.72	2.350	3.120
K_2O	0.185	0.907	0.66	0.36	0.17	1.717	1.190
TiO_2	1.024	1.310	1.09	0.57	0.90	1.086	1.087
P_2O_5	0.105	0.138	0.09	0.09	0.05	0.109	0.102
Total	98.999	101.563	100.83	99.63	99.94	99.781	99.630
Loss	1.01	1.34	0.14	1.41	3.41	5.86	1.25
Ni	274	510	-	-	-	108	54
Cr	1450	1991	856	-	-	136	127
Zn	124	172	-	-	-	205	160
V	232	235	253	-	-	391	337

474: metabasalt Sth. Windarra

478: " " "

40264: metabasalt of Mt. Windarra (Leahey, 1973)

63287: metabasalt of Mt. Hunt (Hallberg, 1970)

P1: Basaltic komatiite (Viljoen & Viljoen, 1969)

135D: dolerite Sth. Windarra

146D: dolerite Sth. Windarra

(2) several samples have high Zn contents (up to 4,300 ppm) reflected in the presence of sphalerite. Pods of both sphalerite and galena form parallel to the layering and these are considered to be sedimentary features.

Metabasalts:

The MgO content (12.5%) of these basalts implies they fall into the "high Mg basalts" of Williams (1971). Compared with the metabasalts analysed by Leahey (1973) at Mt. Windarra they have a similar MgO content however are higher in CaO and lower in Al_2O_3 (see Table 2).

The difference in CaO/Al_2O_3 compared with Mt. Windarra may be a function of either fractionation (Nesbitt, 1971) or alteration.

In comparing the analyses with those of W.A. basalts of a comparable MgO percentage (Hallberg, 1969, Mt. Hunt metabasalt 63287) the metabasalts of Sth. Windarra differ markedly in CaO, Al_2O_3, TiO_2. Here the CaO/Al203 ratio is 1.5 - 1.9 compared with the expected values of Williams (1971) of about 0.82, and those basaltic "komatiites" (Viljoen & viljoen, 1969) at South Africa of 1.67.

When plotted on a diagram of MgO vs Al_2O_3 (see Fig. 7) and compared with the expected trend of Archaean volcanics(Nesbitt, (pers. comm. 1975) it is apparent that most likely Al_2O_3 has been lost. However the presence of abundant epidote in thin sections (see Appendix A) implies CaO enrichment may also be the case.

Granites:

Granites occur both north and south of the greenstone belt, however only analyses of the northern granite were done. Two samples from the intrusion adjacent to the footwall

TABLE 3 ANALYSES OF GRANITES AND FELSITES

	A101	A102	A105	Kambalda Granite	020F	388F	393F	Kambalda Felsite
SiO_2	71.812	72.628	77.002	72.53	72.371	72.259	71.935	72.03
Ai_2O_3	14.938	14.926	13.767	15.70	14.543	15.630	15.126	15.71
Fe_2O_3	2.955	3.371	1.187	1.30	1.455	2.132	1.041	1.50
MnO	0.105	0.120	0.110	0.00	0.027	0.039	0.033	-
MgO	0.799	0.827	0.322	1.54	2.377	2.053	1.995	0.62
CaO	1.457	2.410	0.541	0.48	1.424	2.413	2.057	1.13
Na_2O	4.140	3.630	4.330	5.43	5.21	5.39	5.89	5.56
K_2O	2.626	2.214	2.910	2.19	1.894	1.187	0.877	2.28
TiO_2	0.350	0.349	0.142	0.27	0.195	0.298	0.161	0.31
P_2O_5	0.101	0.071	0.051	-	0.036	0.061	0.004	-
Total	99.278	100.540	100.362	100.02	99.532	101.462	99.119	99.65
Loss	1.20	1.11	2.30	0.44	0.72	0.85	0.80	0.37

A101: northern granite, Sth. Windarra (see Appendix A)
A102: " " " " " " "
A105: intruded granite into ultramafics
020F: Sth. Windarra felsite (see Appendix A).
388F: " " "
393F: " " "
Kambalda granite and Felsite (Ross and Hopkins, 1973).

were taken as well as one sample from the large granitic intrusion in the ultramafics in the west.

Analyses (see Table 3) show considerable variation in the CaO, Na_2O content due to variation in plagioclase composition. When compared with the composition of the Kambalda sodic granite (Table 3), those at Sth. Windarra have more CaO, FeO but less Na_2O due to the higher biotite and calcite plagioclase content.

The granite intruded into the ultramafics differ in composition and mineralogy from the others in that it is less ferromagnesic, more siliceous and has a lower CaO content.

Using the scheme of Harpum, as used by Viljoen and Viljoen (1969), where Na_2O is plotted against K_2O it is clear that the Sth. Windarra granites lie very close to the granodiorites and tonalites of Sth. Africa.

Felsites:

Mineralogically these feldspar porphyries match trondhjemites (Williams, Turner and Gilbert, 1958) but compositionally they plot as tonalites on Harpum's diagram (Viljoen and Viljoen, 1969) based on their high NaO contents (5%) and low K_2O (0.8 - 1.8%). Compared with the sodic rhyolite porphyries at Kambalda (Ross and Hopkins, 1973) they are almost identical, (see Table 3).

Dolerites:

Chemical analyses of dolerites show these to be distinct from other basic rocks of Sth. Windarra (see Table 2). Leahey (1973) has called them meta-olivine dolerites (based on the normative olivine content) at Mt. Windarra and these compare favourably with the Sth. Windarra ones.

<u>TABLE 4</u>

Analyses of the "transgressive ultramafic" (rock types as in Appendix A)
Ni, Cr, Zn, V quoted as ppm, nd = not determined

	A44	A47	350T/Um	360T/Um	484	486	487	488	490	491
SiO_2	45.170	47.291	49.241	50.081	51.052	48.418	46.757	49.837	48.898	43.267
Al_2O_2	5.464	16.854	6.528	5.192	4.608	8.964	10.025	6.568	6.300	8.180
Fe_2O_3	15.920	14.887	10.061	10.845	10.432	12.966	12.215	11.310	14.190	16.348
MnO	0.602	0.289	0.214	0.247	0.248	0.451	0.262	0.455	0.419	0.639
MgO	20.046	10.247	21.415	23.845	23.043	15.733	15.919	17.738	21.171	22.855
CaO	8.063	2.342	6.459	9.104	8.605	8.636	8.174	7.064	9.106	6.519
Na_2O	0.480	1.790	nd	nd	0.320	0.530	0.590	0.300	nd	nd
K_2O	0.049	3.359	4.701	0.078	1.484	2.903	3.145	3.957	0.045	0.023
TiO_2	0.642	1.868	0.582	0.531	0.523	1.032	1.148	0.743	0.736	0.945
P_2O_5	0.068	0.125	0.133	0.053	0.058	0.105	0.118	0.082	0.075	0.082
Total	96.621	99.052	99.334	99.977	100.373	99.738	98.353	98.055	100.913	98.858
Loss	4.58	6.07	1.32	4.20	3.77	1.68	1.49	3.13	4.25	4.35
Cr	2368	424	3305	2463	2409	1780	2139	2292	2965	1899
Ni	871	1.12%	1406	902	961	600	715	734	810	1021
Zn	526	1477	192	99	152	425	308	426	395	589
V	201	334	124	143	133	233	269	202	216	207

Differences do occur, with Sth. Windarra dolerites being more Fe_2O_3 rich and lower in MgO. K_2O is much higher than both the Mt. Windarra ones and Kalgoorlie dolerites (Leahey, 1973).

"Transgressive Ultramafic"

Whole rock analyses are shown in Table 4. The composition of the body is comparable with that of spinifex units however MgO is lower and Al_2O_3 higher. When plotted on graphs of MgO vs Al_2O_3 and MgO vs TiO_2 (Figs. 7 and 8), the "transgressive ultramafic" lies on the fractionation trend defined by the other ultramafics present. It therefore is most likely comagmatic with the spinifex and mineralized units, however was intruded late in the magmatic history of the area.

The large spread of plots also indicates differentiation has been extensive.

Other features are the high K_2O content (up to 4.701%) and Na_2O content. K metasomatism has been intense resulting in the formation of phlogopite while Na_2O represents the presence of feldspars as found in thin section work (see Appendix A).

Trace element work also confirms the similarity of the body to spinifex units. Here Ni is low (up to 1,000 ppm) except for one sample (A47) thought to be anomalous due to shearing and diffusion of Ni. Cr is similar, Zn is higher as is V, (compare with Table 5).

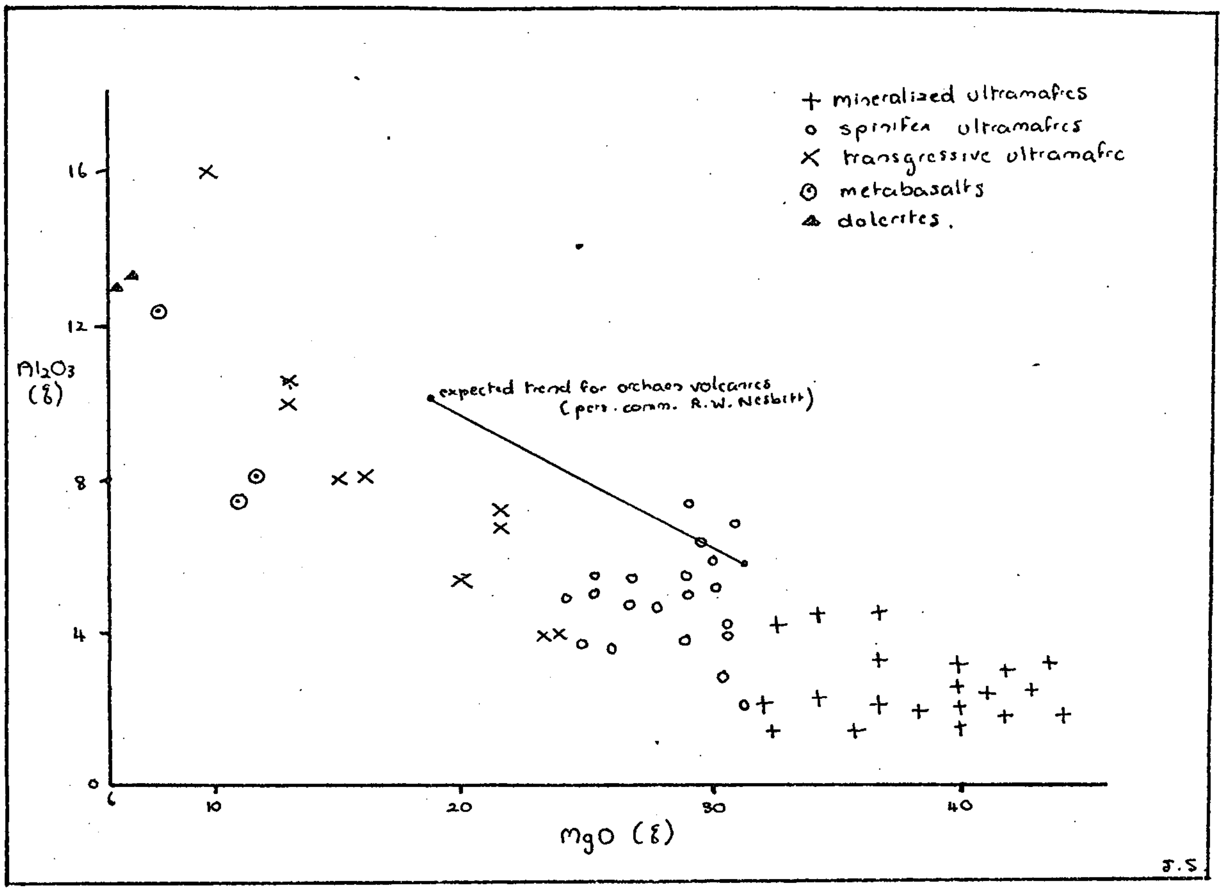

FIG. 7 Plots of MgO vs Al_2O_3 for greenstone assemblages, Sth. Windarra.

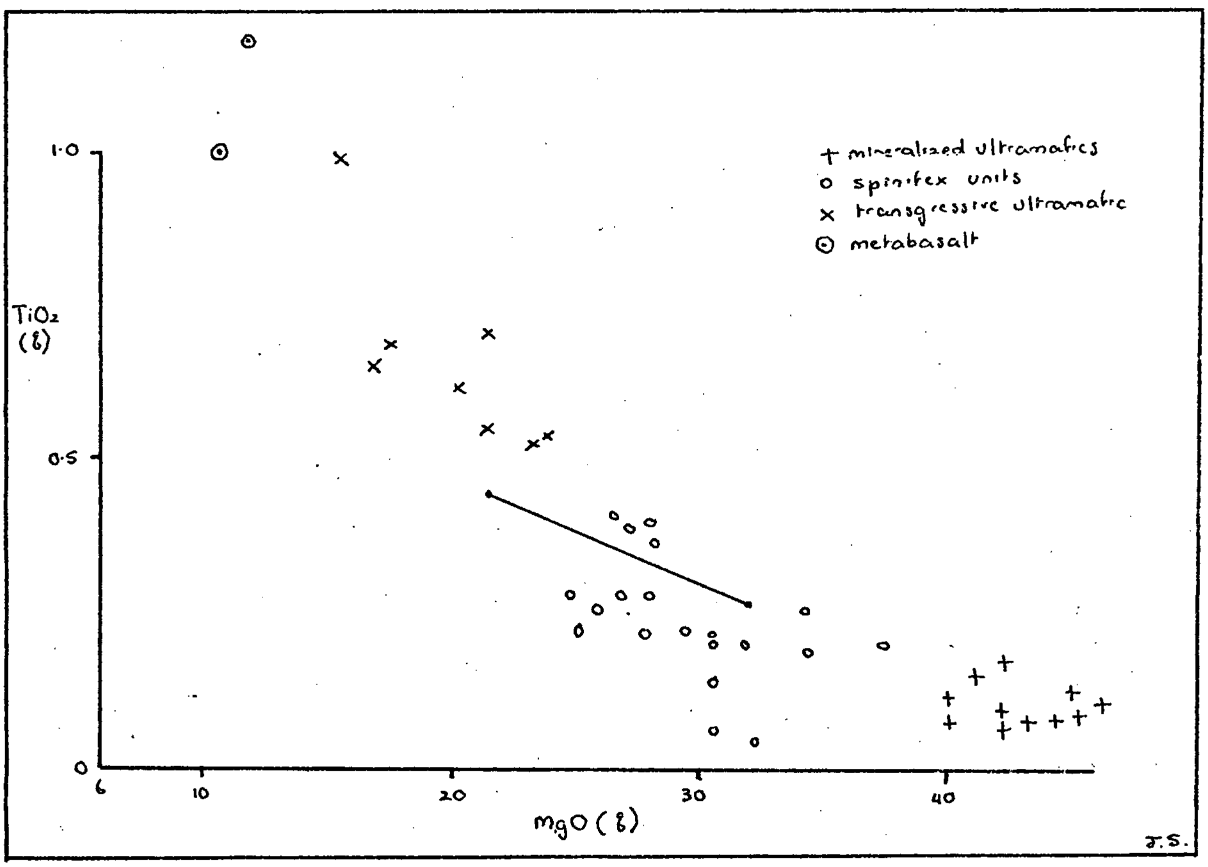

FIG. 8 Plots of MgO vs TiO_2 for greenstone assemblages, Sth. Windarra.

Ultramafics:

(A) Major Element Analyses:

Major element analyses were carried out using standard techniques (see Appendix C). Three drill holes (WSD 23, 93, 100) were representatively sampled on the basis of petrological work, to determine the vertical limits of flow units. The chemical trends and subdivision of flows are shown on two of the drill holes (WSD 93, 100) in Figures 9 and 10, while other data (trace and major elements) are in the Appendix. Drill hole WSD 93 is located in the west of the pit, while WSD 100 occurs in the east.

Trends found across flows are similar to those described by Wilson et al (1969) and Simon (1972). It was however found that out of the elements used by these workers only MgO, and Al_2O_3 were most consistent when comparing trace element data and petrology. CaO, Fe_2O_3 and TiO_2 are useful in distinguishing spinifex ultramafics from ore bearing ones, but do not always conform to trends expected across a flow, due to either metamorphism or complex intrusion.

(a) Mineralized ultramafics:

Magnesia is concentrated towards the centre (reaching up to 44%) but falls off to less than 30% at the margins. Although serpentinization has taken place the trends seen are still valid as suggested by Nesbitt (1971) and Simon (1972) in other serpentinized ultramafics.

The enrichment to the centre (Figs. 9 and 10) is due to an original greater concentration of olivine here, with pyroxene forming at the margins. Thus Alumina shows a negative correlation to Mg. The presence of increased chlorite at margins supports this (see Appendix A).

In both mineralized units Al_2O_3 is commonly $< 3\%$ (excluding margins) compared with the barren spinifex units where Al_2O_3 reaches 8%. A similar comparison can be made for CaO, but due to the mobility of Ca reservations are needed. Stolz (1971) in comparing the Scotia ore bearing unit with overlying ultramafics found spinifex units to be $> 2\%$ while ore units were $< 0.1\ \%$. At Sth. Windarra Ca is highly variable but generalizing, mineralized units have $< 2\%$ CaO, with spinifex ones ranging from 1% to 16% (typical CaO is 6%).

No skeletal zones were found in the mineralized units. Those overlying were not part of the flows but separated by breccias or alteration zones. Hence both mineralized units were composed originally of a crystal mush, with crystals of olivine.

Both mineralized ultramafics are similar in whole rock compositions. Summarizing they have high MgO (up to 44%), low CaO ($< 2\%$), low Al_2O_3 ($< 3\%$) and low TiO_2 ($< 0.2\%$). They are somewhat similar to the massive dunite section of the spinifex units at Scotia as described by Simon (1972), but differ in

(1) they were extruded earlier
(2) no skeletal top exists
(3) they are thicker
(4) trace element contents differ.

(b) <u>Barren Spinifex Ultramafics</u>:

The ultramafic sequence shows an overall decrease in MgO content and increase in CaO, Al_2O_3 content upwards, reflected in the abundance of tremolite/

chlorite up. Of exception is the thin spinifex unit between the mineralized ultramafic, which interrupts the homogenous serpentine rich units.

Geochemically these barren units have a high Mg massive base overlain by a lower Mg, higher CaO, Al_2O_3 skeletal top. They are defined by breccias at the top and bottom plus the following chemical parameters;

(1) CaO is generally 1 - 16%, lower values represent the basal parts.

(2) Al_2O_3 2 - 8%.

(3) MgO ranges from 42% to 21% but more typical values are around 30%.

(4) $TiO_2 > 0.2\%$

These compositions are interpreted as indicating a pyroxenitic nature of the units compared with the more dunitic mineralized units.

Comparisons of typical compositions of the the mineralized units and spinifex units (massive and skeletal zone) occur in Table 5. It is noted that mineralized units have more MgO and less CaO, Al_2O_3 and TiO_2. The difference in composition is thus believed to be due to the fact that most likely the spinifex units fractionated from the massive dunitic mineralized mushes early in the magmatic history. Nesbitt (1971) believes an increasing CaO/Al_2O_3 ratio from mineralized units to spinifex ores reflects this fractionation. Figures 7 and 8 support this idea.

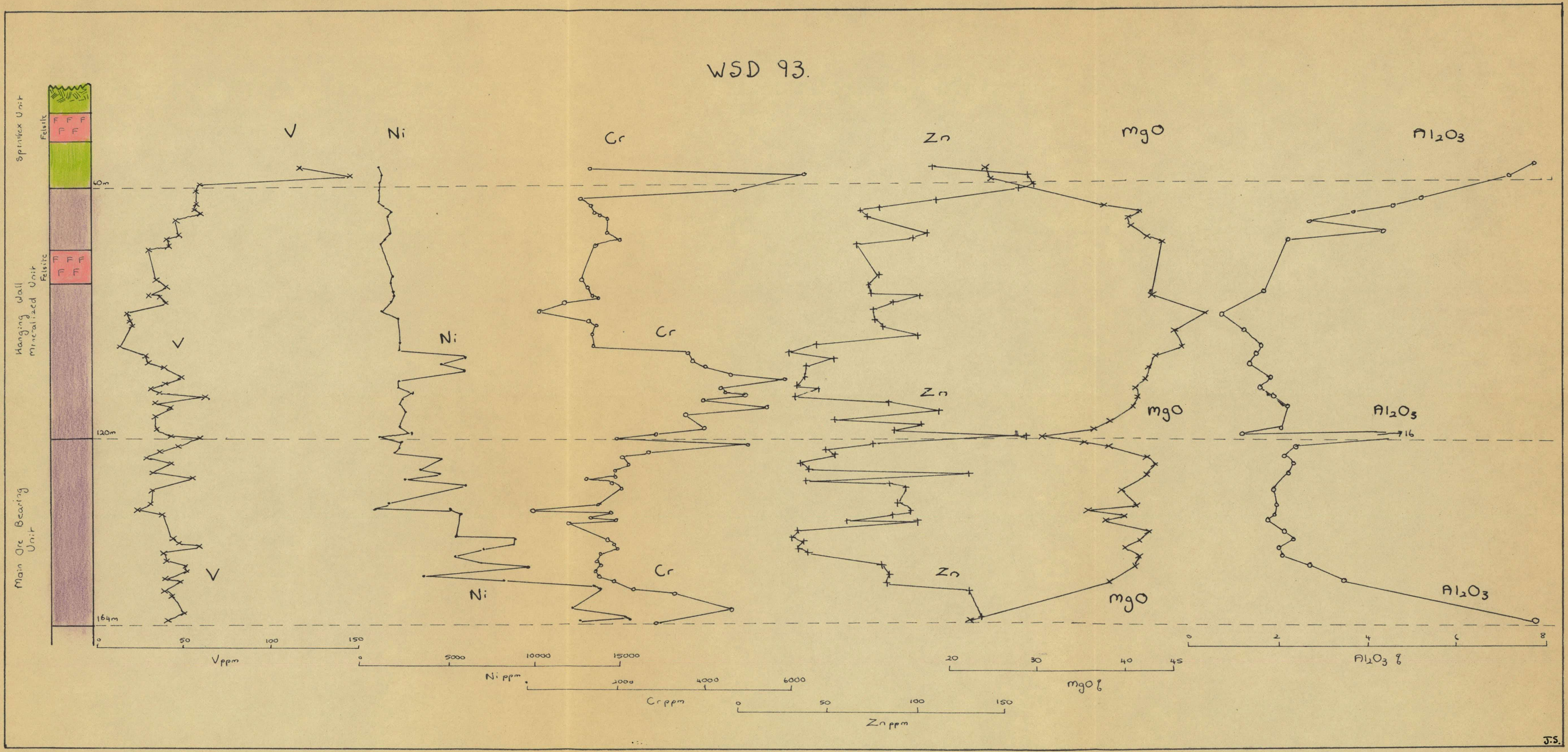

FIG.9 Geochemistry of WSD 93

WSD 100

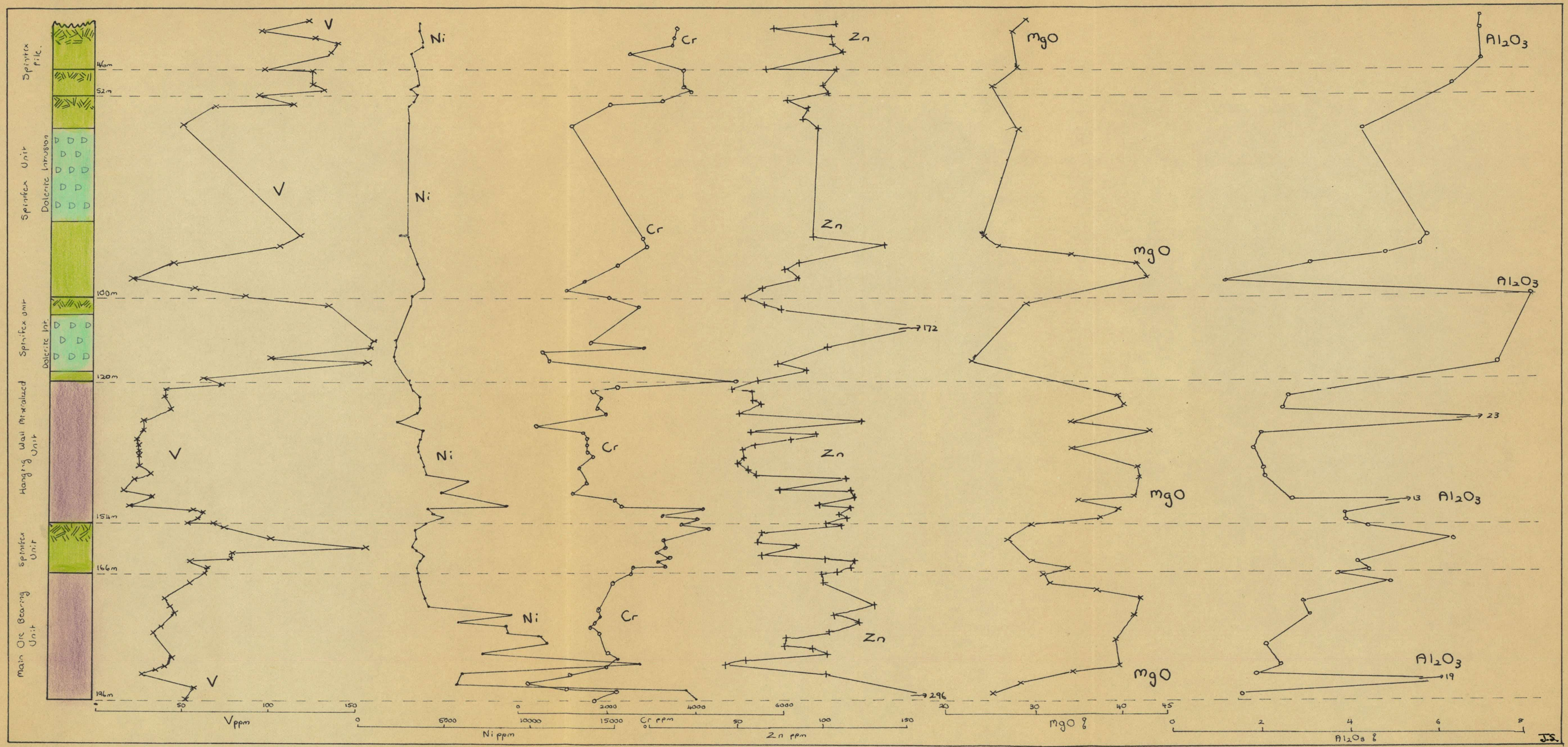

FIG. 10 Geochemistry of WSD100

Of interest, however is the fact that the Sth. Windarra volcanics are depleted in Al_2O_3 compared with the trend expected.

P_2O_5 is generally higher in the mineralized units (most evident in WSD 100, Appendix C) and is thought to be a reflection of the fact that phosphorous shows a tendency to become concentrated in magma fractionation as well as in magmatic sulphides (Rankama, 1949).

TABLE 5

Typical compositions of ultramafic units.

	Ore bearing Unit (233)	Massive barren zone of spinif-ex units (371)	Skeletal Zone (216)
SiO_2	47.108	41.341	48.559
Al_2O_3	2.732	4.396	4.183
Fe_2O_3	7.833	8.889	9.759
MnO	0.115	0.215	0.181
MgO	43.088	35.509	29.612
CaO	0.166	7.768	6.561
Na_2O	-	-	-
K_2O	0.008	0.072	0.050
TiO_2	0.117	0.172	0.214
P_2O_5	0.109	0.051	0.031
Total	101.268	98.348	99.150
Loss	11.72	16.99	8.16

(B) Trace Elements:

Samples were analysed for Ni, Cr, Zn and V using the X-ray fluorescence spectrometer (X.R.F.) as described in Appendix 'D'). Results represent 'total' element abundances (silicate metal content plus sulphide metal content). S was determined using the S titration method as mentioned in Appendix 'D'.

Again these analyses were to primarily outline flow boundaries and supply parameters for distinguishing the two types of units found. Results for two drill holes are presented in figures 9 and 10. Distribution of trace elements supports visual designation of unit boundaries.

(a) Nickel:

Considering the two mineralized serpentine rich ultramafics Ni shows a strong increase towards the base of the flows. This enrichment is thought to be gravitational settling of a denser sulphide-oxide liquid after extrusion, before solidification of the flows.

In the sections studied Ni reaches up to 2% at the base of the main ore bearing unit and drops off over 20 m to about 0.5%, representative of disseminated ore. Massive ore (analysed at Windarra) commonly reached 10%. Near the top of the main ore bearing ultramafic Ni values drop to 0.2% with the alteration zone having low Ni $<$ 1,000 ppm.

The hanging wall mineralized ultramafic shows a similar trend as for the main ore unit but high grades are not as extensive. Ni $>$ 5,000 ppm concentrates at the base over a width of approximately 6 m. Higher values >1% have been found in several holes (WSD104, 91) but due to the small vertical extent, (6m) these concentrations are not economic to mine. Above this basal concentration, values rapidly fall off to 2,000 ppm.

Hence the distinction between the two mineralized ultramafics is the sharp upshoot in Ni content of the base of the hanging wall mineralized unit, from 2,000 ppm to >5,000 ppm. Reservations must be applied since in WSD 93 the Ni concentration of the overlying unit is not at the base but offset, hence all data must be combined to indicate interfaces.

The barren spinifex ultramafics have little or no basal concentration of Ni. Values are <2,000 ppm with exceptions occurring in the spinifex unit between the two mineralized units. Here Ni can reach ore grade (>.8% in WSD 23) in sections close to the hanging wall mineralization. One such example found by D. Cockshell shows sulphides infilling between plates of sheaf spinifex. Because of the high metamorphism, mobility of Ni (breccia and BIF ores), S data (see under Sulphur) and position of the flow under a mineralized unit this Ni concentration is thought to be secondary, from remobilization.

Considering total Ni the barren spinifex ultramafic have similar values to the upper portions of both mineralized units hence resolution of flows on total Ni may be difficult. Stolz on studying Scotia (1971) showed that distinguishing the two types of units of similar total Ni, the sulphide

Ni content was useful, i.e.,

overlying barren units	650 - 850 ppm
ore unit	2,000 - 2,500 ppm

This is possibly the case at South Windarra where polished section work shows very little sulphide content of spinifex barren units.

(b) <u>Chromium</u>:

Chromium trends were found useful as supporting evidence for defining unit interfaces. In general Cr shows a depletion in the centre of both mineralized and barren flows but increases to the margins. Average Cr of mineralized flows is about 2,000 ppm in the centre increasing to 4,000 ppm at the margins. The basal concentration in Cr is thicker than the upper margins. This is thought to be due to concentration of Cr held up in the oxide phase of the sulphide-oxide immiscible liquid, by gravity settling. The existence of coarse chromite grains in the massive ore supports this.

Naldrett and Mason (1968) note that the concentration of chromium increases as the rock grades to pyroxenite from peridotite, as is the case from going from the centre of the flow to the more Al_2O_3 rich margins. Hence generally any significant increase in Cr will mark a flow interface.

Considering the barren spinifex flows, these are defined similarly by Cr trends discussed above. A high Cr value defines the base (3,000 ppm to 6,000 ppm) with Cr decreasing in the massive part to 2,000 ppm. The more pyroxenitic skeletal zones reach values of 4,000 ppm, however for the same type of flow at Scotia, Simon (1972) found values of only 2,000 ppm using atomic absorption.

(c) Zinc

Total zinc exhibits a similar trend to Cr except it increases more towards the top of flows compared with the base. This feature has been found by Ross and Hopkins (1973) at Kambalda and exists in the data of Wilson et al (1969) for the Katiniq sill. The anomalously high values of Zn near the interface of flow units is consistent with sub-aqueous emplacement of a magma (Ross and Hopkins).

As with Cr, Zn data has little use in separating barren units from mineralized ones. Both have an average Zn content of about 50 - 80 ppm with higher values $>$100 ppm at the margins, hence Zn is useful in resolving units. Reservations must be applied due to the mobility of Zn under metamorphism.

Of interest is the high Zn at the base of the main ore bearing unit. This could be a function of Zn tied up in magnetite and chromite concentrated at the base or due to diffusion of Zn from the BIF.

(d) Vanadium:

Vanadium shows an inverse correlation to MgO (Ross and Hopkins), i.e. low Mg spinifex units have a high V content (50 - 150 ppm), high Mg mineralized units and massive sections of barren units have a low V content ($<$ 50 ppm).

Thus in mineralized units V is depleted in the central more Mg rich parts and increases to the pyroxenite margins. The spinifex barren units have a depletion in V in the massive section with V increasing up into the skeletal parts (often $>$100 ppm).

Of note is the slightly higher V content in the main ore bearing ultramafic compared with the hanging wall mineralized unit (50 ppm cf 30 ppm). This can be explained by the affinity of V to substitute for Fe (Rankama, 1949). In the ore bearing unit Fe content is higher due to the presence of pyrrhotite, pyrite, and magnetite.

(e) Sulphur:

Sulphur was determined using sulphur titration methods (Appendix D) in an attempt to show differences in barren and mineralized units.

In both mineralized ultramafics sulphur correlates with Ni i.e. S is highest at the base where Ni concentrates, (values vary from 1,000 ppm to 18%) and decreases up. Stolz (1971) found that at Scotia ore bearing units have a lowest S content of 1,460 ppm while barren units reached 460 ppm. This is the case with spinifex units above the hanging wall mineralization but the unit between the two mineralized serpentinites in the east has substantially higher S (up to 8,080 ppm) at the margins and lower S at the centre (80 ppm). Being between the two high S bearing units it is therefore possible that sulphurization has taken place due to high grade metamorphism.

It is still considered however that S is a useful parameter in locating mineralized units and the value of 1,200 ppm as a divisor for barren and sulphide units, of Stolz is adhered to at Sth. Windarra (exception discussed above).

DISCUSSION

Mineralized ultramafics at South Windarra have contrasting characters when compared with barren spinifex topped ultramafics. The relationship of sulphide mineralization to composition of the ultramafic is important.

It is thought that the mineralized units consisted of a liquid mush of olivine crystals (Barry, 1974) and a high magnesium liquid, and this was hence capable of transporting immiscible sulphide liquids to the surface, i.e. the viscosity was high enough, to sustain sulphides.

The spinifex barren units would have consisted of a similar mush but a higher amount of high Ca, low Mg liquid making it less viscous than mineralized ones. The less viscous nature and sparsity of a large proportion of concentrated crystal mush meant that sulphide immiscible liquids were not able to be carried to the surface, if they were present.

Another important feature is the occurrence of the two mineralized units at the base of the ultramafic pile. If all flows are considered extrusive, then the first liquids to come out were the more Mg rich olivine mushes with sulphides. Following were the more calcic less Mg rich spinifex flows i.e. more fluidous with more liquid resulting in quench spinifex textures (Nesbitt 1971). It then seems plausible to suggest that fractionation by settling in a chamber, of olivine crystals, high Mg liquids and sulphide liquids has taken place, (see page 28).

In comparing barren units with mineralized ores at Sth. Windarra the following features are evident,

	Mineralized units	Barren units
Thickness	40 - 60 m	10 - 25 m
Mineralogy	Wholly serpentine No spinifex	Minor serpentine. Tremolite/chlorite + spinifex textures.
Original liquid	high Mg with olivine crystals i.e. dunitic	high Ca, Al_2O_3 low Mg with minor crystal mush. i.e. pyroxenitic.
CaO	$<2\%$	1-16%
Al_2O_3	$<3\%$	2 - 8%
MgO	$>40\%$	$<40\%$ commonly 30%
S content	$>1,000$ ppm	<300 ppm
Ni	$>2,000$ ppm	$<2,000$ ppm
V	<50 ppm	50 - 100 ppm
Cr	$<2,000$ ppm	$>2,000$ ppm
Zn	50 - 100 ppm	50 - 150 ppm

Most results compare favourably with those found by Stolz (1971) at Scotia with differences noted in Ca which is distinctly higher here in the mineralized units ($<.1\%$ at Scotia). A feature of the study by Stolz is the advantage of determining Ni sulphide fractions to distinguish units. For ore units Ni sulphide $>1,500$ ppm while barren ores are $<1,000$ ppm. This, coupled with the other parameters, especially S provide useful exploration tools.

Of interest is that compared with other major Ni deposits of W.A. two mineralized ultramafics exist at Sth. Windarra indicating that:

(1) not all the sulphide fraction had accumulated in the chamber by the time of the first extrusion.

or

(2) the first ultramafic was unable to hold all the sulphide immiscible liquid.

The existence of the barren spinifex unit between the two mineralized ultramafics has special implications with the fact that composition (content of the magma and amount of liquid) is a controlling feature of sulphide accumulation. Similarly fractionation is also important, in that the spinifex magmas have separated early from the more dunitic magmas and hence sulphide liquids. The presence of this barren unit between mineralized ones therefore probably indicates either:

(1) fractionation was not complete by the time the unit was extruded.

(2) the pulse that brought it up originated higher up in the chamber, away from sulphide immiscible liquids.

(3) or sulphide accumulation in various types of ultramafic magmas depends more on composition (viscosity, liquid compositon) than the process of fractionation, whereby the liquid settles with the higher crystal mushes to the base of chambers.

ACKNOWLEDGEMENTS

The assistance of the following persons and organizations is gratefully acknowledged,

Poseidon Limited, Western Mining Corporation Limited and Windarra Nickel Mines Pty. Ltd. for financial assistance, use of company maps, sections, reports, analytical and drill core data.

John Leahey (Geologist, Samin Limited) and John Roberts, (Chief Geologist, Poseidon Ltd.), for initiating the project and also for helpful discussion and guidance, throughout the year.

Dr. R.W. Nesbitt for helpful supervision and discussion.

Jim Cleghorn (Chief Geologist - Windarra), Dave Cockshell, Derek Judkins and Roger Wright (Geologists - Windarra) for close personal interest in the project, assistance and useful discussion.

Geoff Stolz and Alan Purvis for guidance throughout and discussion on geochemistry. Also for their stimulating ideas.

Rodney Fleeton (Surveyor, Sth. Windarra) for his valued assistance in production of geological mapping, especially in surveying. Also for discussions with Mick O'Brein and Mick Pollock (Mining Engineers).

Staff and fellow honours students.

David Bruce and Lee Collins for fused buttons, Na analyses and supervision of running of geochemical samples.

Margy Wright for X.R.D. work, Keith Turnbill for S analyses advice.

Laboratory staff for preparation of thin and polished sections, and not to forget the typist, Marilyn O'Loughlin for the large amount of time that has gone into production.

-o-0-o-

REFERENCES

BARRY, J., 1974. Geochemistry of the Scotia Nickel Deposit in relation to exploration. Unpublished Ph. D. Thesis, University of Adelaide.

BAXTER, D.R., 1971. The Petrology and Geochemistry of an Ultramafic body near Ravensthorpe, Phillips River Goldfield, W.A. Unpublished B.Sc. Honours thesis, Adelaide University.

BOWEN, N.L., and TUTTLE, O.F., 1949. The System $MgO-SiO_2-H_2O$. Geol. Soc. America Bull., 439 - 460.

COLEMAN, R.G., 1971. Petrologic and geophysical nature of serpentinites. Geol. Soc. Am. Bull., 82:897-918.

COLEMAN, R.G., and KEITH, T.E., 1971. A Chemical Study of Serpentinization - Burro Mt., California. J. Petrology, 12 : 311 - 328.

DAVIDSON, J.E., 1970. A Petrological and Geochemical Study of three Diamond Drill Holes through the Mt. Windarra Ultramafics and Zone of Mineralization. Unpublished B.Sc. Honours thesis, Adelaide University.

DRAKE, J.R., 1972. The Structure and Petrology of Banded Iron Formations at Mt. Windarra, W.A. Unpublished B. Sc. Honours thesis, University of W.A.

DREW, G.J., 1971. A Geochemical Study of the Weathering Zone at Mt. Windarra, W.A. Unpublished B. Sc. Honours thesis, Adelaide University.

ECKSTRAND, O.R., 1975. The Dumont Serpentinite: A Model for Control of Nickeliferous Opaque mineral Assemblages by alteration reactions in Ultramafic rocks. Eco. Geology, 70 : 183 - 201.

EVANS, B.W., and TROMMSDORF, V. 1974. On Elongate Olivine of Metamorphic origin. Geology, 2 : 131 - 132.

EWERS, W.E., 1971. Nickel-iron exchange in pyrrhotite. Aust. Inst. of Min. and Metall. Annual Conf. N.Z. Paper No. 14.

EWERS, W.A., and HUDSON, D.R., 1972. An interpretive study of a nickel-iron sulphide ore intersection Lunnon Shoot, Kambalda, W.A. Econ. Geol. 67 : 1075 - 1092.

GROSS, G.A., 1965. Geology of Iron Deposits in Canada, Vol. 1 Econ. Geol. Sect. Can., 22.

GROVES, et al, 1975. AMIRA Research Project. Various reports University of W.A.

References (Continued)

HALLBERG, J.A., 1970. The Petrology and Geochemistry of Metamorphosed Archaean basic volcanic rocks between Coolgardie and Norseman, W.A. Unpublished Ph. D. thesis, University of W.A.

HESS, H.H., 1933. The Problem of Serpentinization and the Origin of Certain Chrysotile Asbestos talc and Soapstone deposits. Econ. Geol. 28, 634 - 675.

HUDSON, D.R., 1972. Evaluation of Genetic Models for Aust. Sulphide Nickel Deposits, Aust. Inst. Min. Metall. Conference, Newcastle: 59 - 68.

HUDSON, D.R., 1973. Genesis of Archaean Ultramafic - Associated Nickel-iron Sulphides at Nepean, W.A. Aust. Inst. Min. Metall. Conference, W.A. 99 - 109.

JAHNS, R.H., 1976. Serpentinites of the Roxbury District, Vermont. Ultramafic and Related Rocks. Ed. Wyllie, P.J., 137 - 155.

KILBURN, L.C. et al, 1969. Nickel Sulphide ores related to ultrabasic Intrusions in Canada. Econ. Geol. Monograph 4 "Magmatic Ore Deposits", 276 - 293.

LEAHEY, J.E., 1973. The Geology and Nickel-Copper Mineralogy of the D-shoot, Mt. Windarra, W.A. Unpublished B.Sc. Honours Thesis, University of Tasmania.

MACLEAN, W.H., 1969. Liquidous Phase Relations in the FeS -FeO- Fe_3O_4 - SiO_2 system and their application in Geology. Econ. Geol. 64 : 865 - 884.

NALDRETT, A.J., 1967. Talc-carbonate Alteration of some Serpentinized Ultramafic Rocks South of Timmins, Ontario. J. Petrology, 7 : 489 - 499.

NALDRETT, A.J., and GASPARRINI, E.L., 1971. Archaean nickel Sulphide Deposits in Canada : their classification, geological setting and genesis, with suggestions as to Exploration. Geol. Soc. Aust. Spec. Pub. 3.

NALDRETT, A.J., and MASON, G.D., 1968. Contrasting Archaean Ultramafic Igneous Bodies in Dundonald and Clergue Townships, Ontario. Can. Jour. Earth Sci., 5 - 1; 111 - 143.

NESBITT, R.W., 1971. Skeletal Crystal Forms in the Ultramafic Rocks of the Yilgarn Block, W.A.; evidence for an Archaean Ultramafic Liquid. Geol. Soc. Aust.S.P.3.

NORRISH, K., and HUTTON, J.J., 1968. An Accurate X-Ray Spectrographic Method for the Analysis of a Wide Range of Geological Samples. Geochem. et Cosmochim. Acta, 33 : 431 - 453.

OLIVER, R.L., et al, 1972. Metamorphic Olivine in Ultramafic Rocks from W.A. Contrib. Mineral. and Pet. 36 : 335 - 342.

PYKE, D.R. et al, 1973. Archaean Ultramafic Flows in Munro Township, Ontario, Bull. Geol. Soc. Am. 84 : 955 - 978.

RANKAMA, K., and SAHAMA, T.H.G., 1949. Geochemistry. (The University of Chicago Press).

ROBERTS, J.B., 1974. Nickel Deposits at Windarra, W.A. To be Published in Econ. Geol. of Australia and Papua New Guinea.

ROBINSON, W.B. et al, 1973. The Discovery and Evaluation of the Windarra Nickel Deposits, W.A. Aust. Inst. Mines Met. W.A. Conf. 69 - 90.

ROSS, J.R., and HOPKINS, G.M.F., The Nickel Sulphide Deposits of Kambalda, W.A. To be Published in Econ. Geol. of Australia and Papua New Guinea.

SIMON, I.K., 1972. A Geochemical and Petrological Investigation of the Massive Dunite Members of the Scotia Ultramafic Belt. Unpublished B. Sc. Honours Thesis. Adelaide University.

SKINNER, B.J., and PECK, D.L., 1969. An Immiscible Sulphide Melt from Hawaii. Econ. Geol. Monograph 4 : 310 - 322.

STOLZ, G.W., 1971. The Petrology, Mineragraphy and Geochemistry of the Nickel Ore Zone and Host Ultramafic Rocks at Scotia, W.A. Unpublished B. Sc. Honours Thesis. University of Adelaide.

VILJOEN, M.J., and VILJOEN, R.P., 1969 : Upper Mantle Project, Special Publ. 2, Geol. Soc. S. Af.

WATCHMAN, A.L. 1971. A Study of Two Geological Sections and the Petrology and Geochemistry of the Ultramafic Rocks - Mt. Windarra Ore Body, W.A., Unpublished B. Sc. Honours Thesis. Adelaide University.

WILLIAMS, D.A.C., 1971. Determination of Primary Mineralogy and Textures in Ultramafic Rocks of Mt. Monger, W.A. Spec. Pub. Geol. Soc. Aust. 3 : 259 - 268.

WILLIAMS, H., TURNER, F.J., and GILBERT, C.M., 1958. Petrography (Freeman and Co.)

WILSON, H.D.B., et al. 1969. Geochemistry of Some Canadian Nickeliferous Ultrabasic Intrusions. Econ. Geol. Monograph 4 : 294 - 309.

-o-0-o-

Plate 1

Figure a: Near vertical large dolerite intrusion, intruded by a thin felsite emplaced later.

Figure b: vertical feldspar porphyry dyke.

Figure c: dolerite intrusion lensing out with depth.

PLATE I

a

b

c

Plate 2

Figure a: Alteration of pyrrhotite by flames of violarite extending in from the margins of grains. Finer grains are violarite while the coarse grain is pyrite.

Figure b: Pyrite porphyroblasts sitting in a matrix of essentially pyrrhotite (massive ore).

Figure c: Strands of pentlandite form layers with silicates. Violarite alteration is common on margins of grains.

Figure d: Equant even grained violarite with weak relict pentlandite. Violarite flames are replacing pyrrhotite from the margins.

PLATE 2

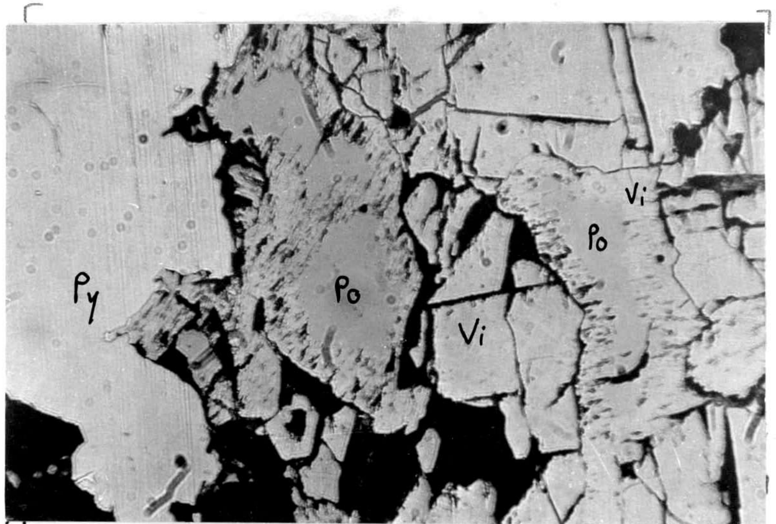

a

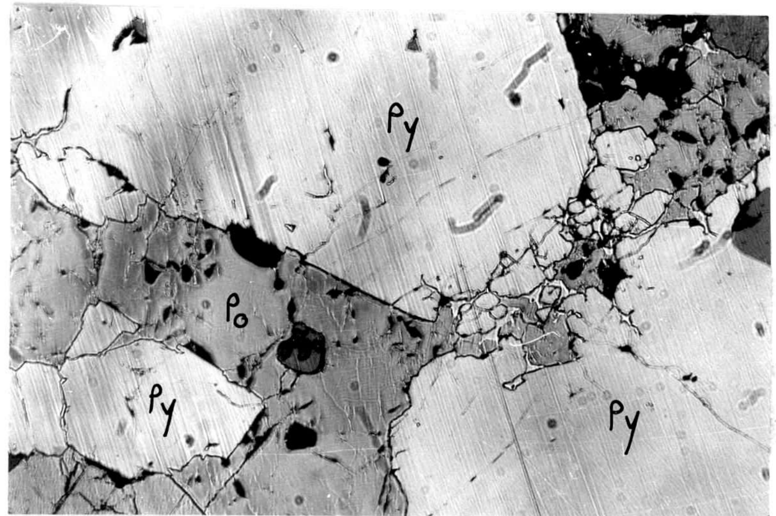

b 160X

c 56X

missing

d 160X

Plate 3

Figure a: Coarse megacrysts of serpentine amongst a fine matrix of feathery serpentine and chlorite.

Figure b: equant close packed serpentine grains.

Figure c: spinifex texture (random) with elongate areas of chlorite in a ground mass of tremolite.

Figure d: Needles of tremolite in a matrix of fine chlorite from overlying barren spinifex units.

PLATE 3

a

b

Missing

0 —— 1mm

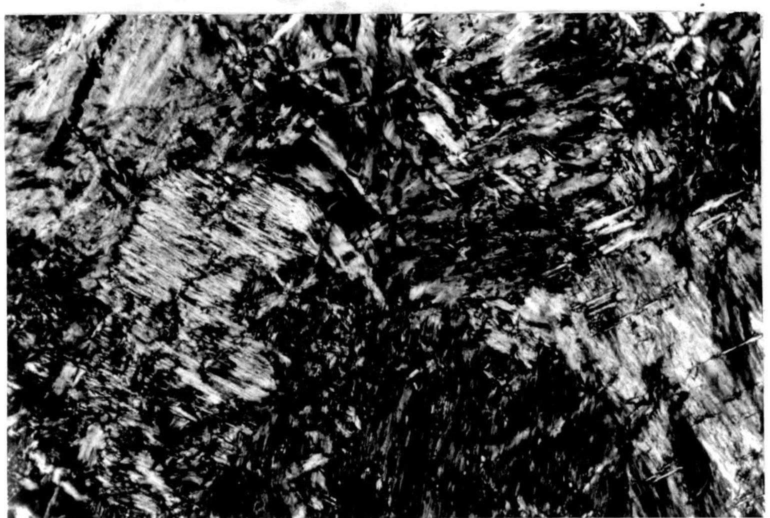

c

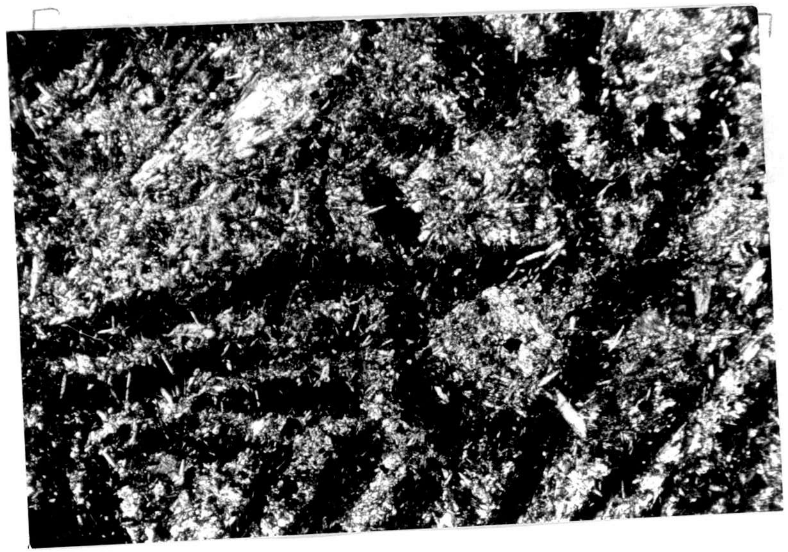

Plate 4

Figure a: "Transgressive ultramafic" with elongate fine quartz amongst fibrous biotite and chlorite.

Figure b: Feldspar porphyry. Phenocrysts of original igneous zoned plagioclase sit in a fine matrix of quartz and biotite.

Figure c: Dolerite intrusion. Xenoblastic quartz and feldspar between interlocking blades of hornblende.

Figure d: Granite. Lepidoblastic biotite and muscovite surround composite grains and aggregates of quartz and feldspar.

PLATE 4

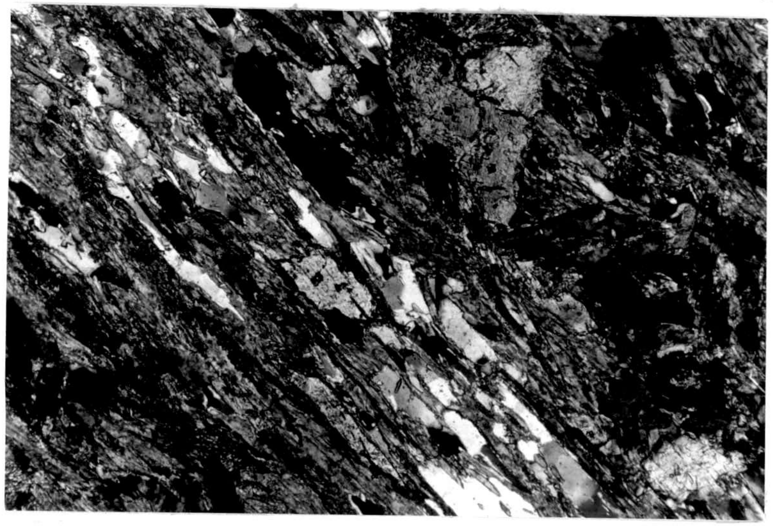

a

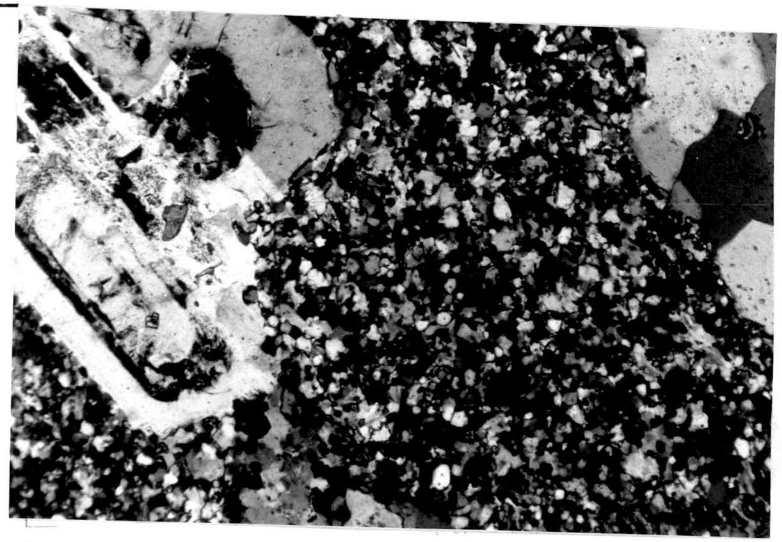

b

0 1mm

c

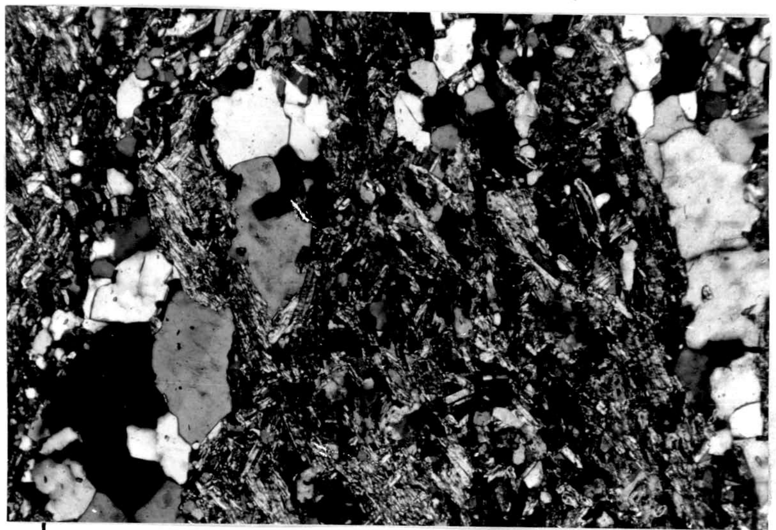

d

Plate 5

Fig. A:	Sheaf spinifex
Fig. B:	Alignment of porphyroblastic olivine under spinifex textures.
Fig. C:	Breccia at the top of a spinifex unit.
Fig. D:	Breccia ore at the contact of metasediment and ultramafic (chlorite schists amongst banded pyrite).

PLATE 5

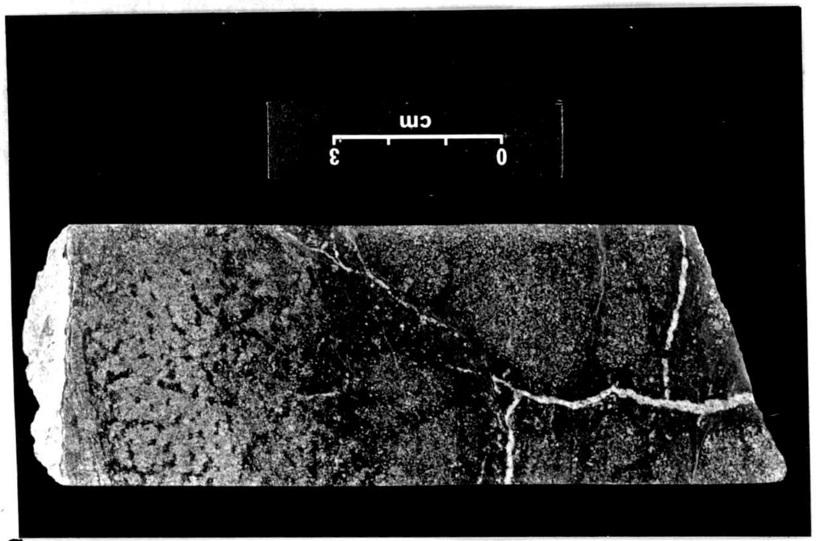

a

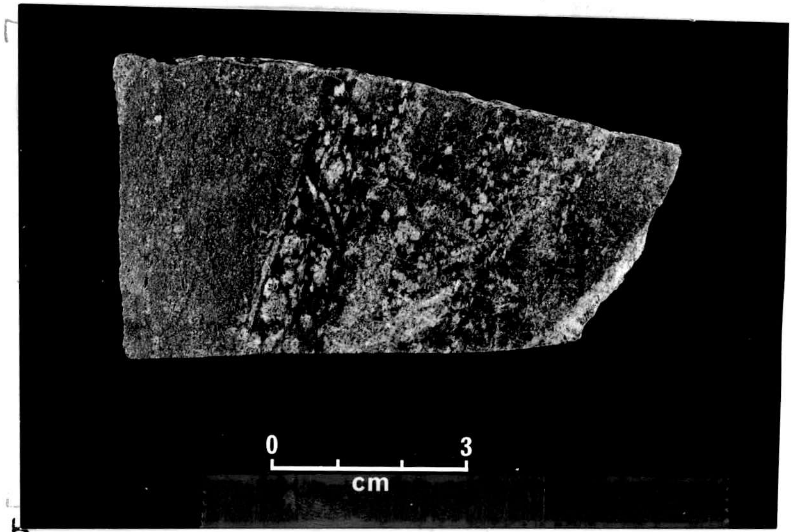

b

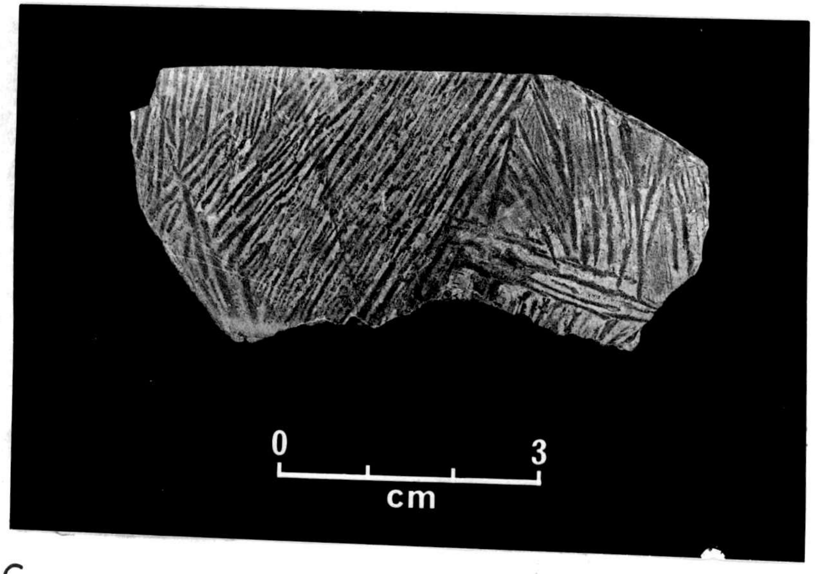

c

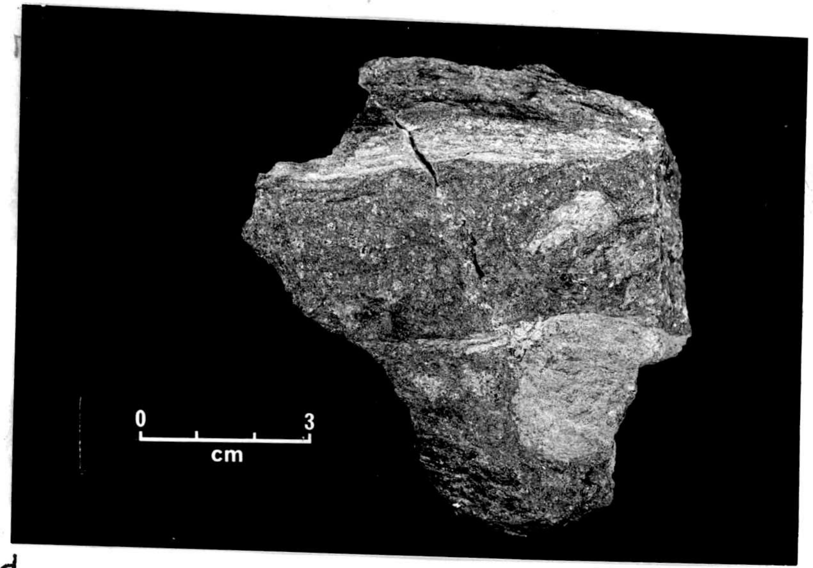

d

APPENDICES

Petrography

Appendix A: Thin Sections (modal analyses)

Appendix B: Opaque Mineralogy (descriptions, modal analyses).

Geochemistry

Geochemical sections.

Appendix C: Whole Rock Analyses

Appendix D: Trace Element Analyses

APPENDIX A

Thin Sections (modal analyses)

THIN SECTIONS

Where S = serpentine, Tr = tremolite, Tc = talc,
Ch = chlorite, C = carbonate, Op = opaques).

WSD 93

Sample No.	Distance down hole (m)	S	Tr	Ch	Tc	C	Op	Textures & comments
001	56		87	10	1		2	Chlorite fibrous aggregates in a fine-grained tremolitic matrix.
002	58		93	2			5	Fine needles of tremolite are aligned to form a schistosity.
003	59		78	T	10	2	10	Porphyroblastic magnetite in fibrous tremolite.
006	64			80	15		5	Schistose chlorite
008	65.5	40			55		5	Talc alteration is strong.
009	66	50			45		5	" " " "
010	67	55			40		5	Even grained serpentine.
011	68	40			20	30	10	Weakly schistose
012	69	50			20	20	10	Uneven grained serpentine.
013	70	50			30	10	10	" " " "
014	71	50			5	40	5	Talc-carbonate alteration is strong.
015	72	50			10	35	5	" " " "
028	86	55			10	25	10	Weakly schistose
033	90	60			2	30	8	Coarse aggregate of fibrolamellar serpentin moderately carbonated.
035	92	50		1	2	40	7	Coarse (3-7mm) lamellar serp.
038	94	70			10	10	10	Fine leaflike fibrous serpentine.
044	99	75			5	10	10	Equant coarse grained serpentine outlined by magnetite.
047	100	75			5	10	10	Even grained serpentinite.

WSD 93 (Continued)

Sample No.	Distance down hole (m)	S	Tr	Ch	Tc	C	Op	Textures & Comments
050	103	70		5		10	15	Even grained serpentinite.
053	105	75		10			15	Chloritic serpentinite
058	110.5	60		5		5	30	Fibrolamellar serpentine grains interlock with opaques.
060	112	60		5		5	10	Coarse serpentinite
064	118	60				5	15	" " "
065	119	20		5	75		10	Talc breccia
066	120			83	15		2	Coarse blades of chlorite interlock to form a coarse aggregate.
067	120.1	60		2		3	35	Coarse prisms of serpentine.
069	123	70		5	10	5	10	Megacrysts of serpentine sit in a fine matrix of chlorite and serp.
071	126	80		5		2	10	" " " "
073	128	80		10			10	Chloritic serpentinite
076	132	87		5		3	5	Coarse lamellar serpentine grains interlock.
078	136	85				5	10	Even grained serpentinite
080	138	75			5	10	10	" " "
081	139	80				10	10	" " "
083	141	50		10		30	10	Chloritic serpentinite with megacrysts (3 - 4 mm) of serp.
084	144	70		5		5	20	Even grained.
086	146	70		10		8	12	Coarse lamellar serpentine defined by opaque trails.
087	147	80		5			15	" " "
089	151	73		10		5	12	Feathery serpentine. Uneven grained.
091	152	50			10	25	10	Carbonated serpentinite

WSD 93 (Continued)

Sample No.	Distance (m)	S	Tr	Ch	Tc	C	Op	Textures & Comments
093	156	20				60	20	Carbonated serpentinite
100	164			5	45	30	15	Talc-carbonate schist.

WSD 100

Sample No.	Distance (m)	S	Tr	Ch	Tc	C	Op	Textures & Comments
110	31		60	30	5		5	Spinifex textures evident.
113	34		70	25			5	Blades of chlorite form a schistosity.
118	44		55	40			5	" " " "
122	49		60	35			5	" " " "
125	52		60	35			5	" " " "
127	54		55	40			5	Fine needles and flakes of tremolite and chlorite interlocking.
130	58		40	55			5	Chlorite aggregates abundant.
150	80		35	30	30		5	Talc, tremolite blades sit in a matrix of fibrous chlorite.
153	86		35	35	25		5	Talc/tremolite schist.
155	88		30	40	25		5	" " "
158	93	85		2	10		3	Slightly schistose serpentinite.
161	97	32			55	10	3	Fibrous serpentine sits in a matrix of carbonate and talc.
165	101		60	37			3	Tremolite/chlorite schist.
179	116		60				5	Phlogopite 35%.
185	122	75			10	5	10	Coarse lamellar serpentinite.
189	127	75				15	10	" " "

WSD 100 (Cont.)

Sample No.	Distance (m)	S	Tr	Ch	Tc	C	Op	Textures & Comments
192	130			95			2	Chloritic schist with apatite 3%.
194	132	80			5	5	10	Even grained serpentinite.
196	134	70			10	10	10	" " " "
200	139	80				10	10	Lamellar serpentine, thatched.
207	148	80				5	15	" " "
208	149			80			20	Magnetite chlorite schist.
210	150	50		40			10	Equant serpentine.
213	152	70			5	5	20	" "
216	156		30	55	10		5	Spinifex textures evident.
217	158		30	50	10		10	Tremolite/chlorite schist.
222	163		65	33			2	" " "
224	164	30	35	5	10	5	15	Altered serpentinite with tremolite needles in a serpentine matrix.
226	166			90			10	Chloritic schist.
227	167	25	30	10	3	20	12	Tremolitic serpentinite
233	172	55		25		15	15	Interlocking grains of medium serpentine.
236	173	80				5	15	Coarse serpentinite.
241	181	83				2	15	" "
246	186.5	70				5	25	" "
250	189	73				2	25	Equant serpentine.
251	190	55			15	5	25	" "
252	193		20	77			3	Tremolite/chlorite schist.
253	195		45	10	15		30	" " "
256	197		35	5	25		35	Sulphide rich contact schist.

WSD 23

Sample No.	Distance (m)	S	Tr	Ch	Tc	C	Op	Textures & Comments
345	47		50	40			10	Spinifex texture with fibrous chlorite enclosing tremolite needles.
347	48		90		T		10	Tremolite coarse blades form parallel sets.
354	56		10	60	10		10	Fibrous chlorite
364	72		40	25	30		5	Uneven grained tremolite/chlorite schist.
367	77		65	30			5	" " " "
372	87	15		30	35	15	5	Talc/carbonated serpentinite.
375	92		20	60	15		5	Tremolite/chlorite schist.
380	99		25	45	25		5	Alternating layers of chlorite and tremolite.
382	103		65	35			5	Tremolite/chlorite schist.
386	107		55	15			T	Phlogopite 30%
391	116		15	30	35		10	Talcified tremolite/ chlorite schist with euhedral magnetite.
396	124			40	30	25	5	Talc/carbonated chlorite schist.
399	129	75			5	15	5	Moderately carbonated serpentinite with a schistosity formed by carbonate trails.
401	131		25		72		3	Talc schist, steatite rock.
403	136	90				3	7	Coarse serpentine amongst finer thatched serpentine.
410	147	90		5			5	" " " "
417	158	95					5	Coarse grained serpentinite.
423	170	78		2		10	10	Uneven grained.
428	173		50	30	15		2	Talc/tremolite/chlorite schist.

WSD 23 (Cont.)

Sample No.	Distance (m)	S	Tr	Ch	Tc	C	Op	Textures & Comments
432	179		35	55			5	Fibrous tremolite amongst chlorite.
433	181		5	75		15	5	Flaky chlorite interlocking serpentinite.
440	191	60		25			15	" " " "
442	193	66		20	6		8	Talcose serpentinite.
443	194	30			60		10	" "
447	198			93	4	1	2	Highly chloritic schist
452	204		3		87		10	Steatite
454	206	75		2		8	15	Weakly carbonated serpentinite.
457	211			20			5	Phlogopite 75%
460	216	47		3	10	30	10	Talc/carbonated serpentinite.

BANDED IRON FORMATIONS

(Where Q = quartz, G/C = grunerite/cummingtonite,
Hb = hornblende, Ac = actinolite, Op = Opaques,
C = carbonate, Bi = biotite, G = garnet,
Ap + S = apatite and sphene).

Sample No.	Q	G/C	Hb	Ac	Op	C	Bi	G	AP + S	Comments
105	65	20			15				T	Layering present.
106	70	25			10	5		T		Alternating layers of amphibole and quartz.
258	50	20			10	15			5	Carbonate alteration highly recrystallised, near contact.
302(2)	40				10	25	25			" " " "
303	70				15	10	5		T	
309	50	20	15		10				5	Alternating layers of differing grain sizes.
337	45	20	5		15	2	15			
342	40	30			20	T	10		T	
464	5			60	35					Highly stained

BANDED IRON FORMATIONS (Continued)

Sample No.	Q	G/C	Hb	Ac	Op	C	Bi	G	AP +S	Comments
469	40	50		T	8	T			2	
473	35	55			10				T	Xenoblastic quartz alternates with coarser grained amphiboles.
B100	5				10		60	25		Garnet porphyroblasts.
482	35		20		15		30		T	BIF amongst metabasalts

META BASALTS

(Where Q = quartz, P = plagioclase, Ac = actinolite, Bi = biotite, S = sphene, E = epidote, Hb = hornblende, Op = opaques).

Sample No.	Q	P	Ac	Hb	Bi	Op	E	S	Comments
474	10	5	70				7	8	Medium actinolite interlocks to form laths, infilled by Q and P.
476	20	5	5		30	5	30	5	Epidote alteration is high.
478	10	10	45		20	5	5	5	Biotite replacement common.

DOLERITES

Sample No.	Q	P	Ac	Hb	Bi	Op	E	S	Comments
135D	15	15		65		5	T	T	Amphibolite
146D	20	5		70		2	1	2	Interlocking Hb forming laths.

"TRANSGRESSIVE ULTRAMAFIC"

(Where Q = quartz, F = feldspar, Bi = biotite,
Tr = tremolite, Ch = chlorite, C = carbonate,
Tc - talc, Op - opaques, Act = actinolite,
Acc = accessories, Hb = hornblende).

Sample No.	Q	F	Bi	Tr	Ch	Tc	C	Op	Act	Hb	Acc
484			45	50				5			
485					25	59	10	6			
486	15	5	30		15			3	30		2
487	20	5	35		5					30	5
488	10	5	35					5	40		5
489				60	35			5			
490				50	45			5			
491				42	50			3			5
492			25	20		35	20				
A44				40	45			15			
A45	5	5	10		20			10		50	
A47	25	5	35		30						5
A48	10			10	15	40	15	10			
350 T/um			45	50				5			
360 T/um				10	25			10		35	

GRANITES

(Where Q = quartz, Kf = K feldspar, P = plagioclase,
Bi = biotite, Acc = accessories, Ch = chlorite,
M = muscovite, Op = opaques)

Sample No.	Q	Kf	P	Bi	M	Ch	Op	Acc	Comments
A101	20	10	40	8	20	2		T	Uneven grained, alteration of Bi to ch
A102	30	5	10	10	35	5	3	2	Fibrous muscovite surrounds coarser feldspar and quartz.
A105	40	10	30		20				Coarse feldspar and quartz set in a fine matrix.

FELDSPAR PORPHYRY DYKES

Sample No.	Q	Kf	P	Bi	M	Ch	Op	Acc	Comments
020F	40	5	40	2		10	T	1	Porphyroblastic texture with feldspar grains in a fine matrix.
393F	45	5	35	8		2	2	3	" " " "
388F	40	5	40	5	5	3	2	T	" " " "

APPENDIX B

Opaque mineralogy (descriptions, modal analyses).

OPAQUE MINERALS

(Where: Pn = Pentlandite, Po = Pyrrhotite,
Py - Pyrite, Mag = Magnetite, Mi = millerite,
Cy = Chalcopyrite and Chr = Chromite,
T = trace, U/m = ultramafic).

Massive Ore (representative sample 451/100)

Texture: Sulphides and magnetite account for 70% of the polished section with the main sulphides including coarse grained equant subidiomorphic pyrite, elongate pyrrhotite, violarite plus minor chalcopyrite and pentlandite. Most grains, except pyrite are xenoblastic.

Pyrite: Occurs as both coarse (3mm) and fine grained euhedral and subhedral porphyroblasts. The coarser subhedra form py rich layers with interspersed Po and Vi. These have spongy contacts with silicates but when in contact with Po show straight contacts. Smaller grains (0.2 mm) have a similar habit and often form as interlocking masses with Po and Vi. Inclusions of Cy and Po are common.

15%

Magnetite: forms as fine grained anhedra (0.5 mm) in both sulphide and silicate rich areas. The majority of grains associated with sulphides have chromite cores.

10%

Pyrrhotite: tightly welded xenoblastic aggregates form elongate masses with violarite. Finer blebs occur in the silicate rich areas. Generally most Po grains show violarite exsolution flames plus alteration to violarite at the edges in contact with the Ni rich mineral. Small elongate lots of Po, Vi also occur.

40%

Violarite: equant fine grains (0.15mm) interlock with Po. Several of these show relict pentlandite present. Vi is common as an alteration product on edges of adjacent Po or as exsolution flames in Po.

33%

Massive Ore (Continued)

Chalcopyrite: subhedra and anhedra are generally associated with pyrite.

2%

Disseminated Ore (451/091)

Texture: most of the sulphides are matrix to the silicate minerals forming around grains, along boundaries. The grains are very fine and often cracked and corroded. Sulphides and magnetite constitute 30% of the rock with the main minerals being mag, Po, Py, Vi and minor Cy. Violarite (no relict Pn) forms coarse aggregates, while most other grains show a linear feature (shearing) through them.

Pyrrhotite: minor pyrrhotite occurs with violarite as relict cores after extensive alteration to Vi from the edges. Other fine subhedra exist with pyrite, while several grains also form amongst more bleby pyrite

15%

Violarite: corroded sheared grains (up to 1 mm) exist with magnetite around silicate hosts. No relict Pn can be seen, however minor Po after Vi alteration is found.

35%

Magnetite: magnetite occurs either as medium grained subhedra with violarite, around silicate boundaries or as very fine anhedra scattered throughout the section.

20%

Pyrite: most grains are euhedral associated with silicates however others in contact with sulphides have a bleby nature with corroded edges.

20%

Chalcopyrite, Millerite: both occur as fine subhedra amongst Po grains.

10%

HOLE WSD 93

Sample	Position (m)	U/m	% Opaques	Pn	Vi	Po	Py	Mag	Cy	Mi
012	70		2		T		35	65		
043	99	Hanging	10		5		45	50		
050	103	Wall	25		5		45	50		
058	110	mineral-	15		5	5	40	50		
061	114	ised U/m	15		5		30	65		
067	120		20		30		T	70		
076	132		20		20		40	40	T	
078	136		25		50		T	50	T	
079	137		5		T		50	50	T	
081	139	Main	25		35		20	40	5	
084	144	Ore	30	10	25	5	25	35	T	
090	151	Unit	30		40	15	25	20	T	T
091	153		30	T	35	15	20	20	5	5
093	156		60	10	45	35	10	3	2	
094	157		70	15	20	50	5	5	3	2
097C	161		60	9	30	50	T	10	1	
097B	161.5		90	10	10	38	35	5	2	
097A	162		95		3	2	95	T	T	
100	164		70	5	30	40	15	10	T	
105	167	BIF	30			49		50	1	
106	169		20			10	2	87	1	

HOLE WSD 100

Sample	Position (m)	U/m	% Opaques	Pn	Vi	Po	Py	Mag	Cy	Mi
158	93	Spinifex	3		T	85	T	15		
164	100	U/m	8		5	25	30	40		
188	125		10		T	50		50	T	
194	132	Hanging	10	40	T	T		60		
204	145	Wall min-	10	60		T		40		
205	146	eralised	10	50		15		35	T	
208	150	U/m	60		5		30	65		
210	151		10	20			30	50		
214	153		15	15		20		60	5	
216	156		10	28				70	2	
219	160		5	50				50		
222	163	Spinifex	15	10		55		30	5	
223	164	U/m	5	10		55		30	2	3
226	166		10	15		50		30	5	
228	168		20	30		15		50	3	2
232	171		30	40		35		40	5	
242	182	Main Ore	25	20	8	30		40	2	
249	189	Unit	25	15		45	3	35	2	
250	192		30	30	3	35		30	2	
254	195		60	40		50		10		
256	196		70	30	T	70				

GEOCHEMICAL SECTIONS

WSD 23.

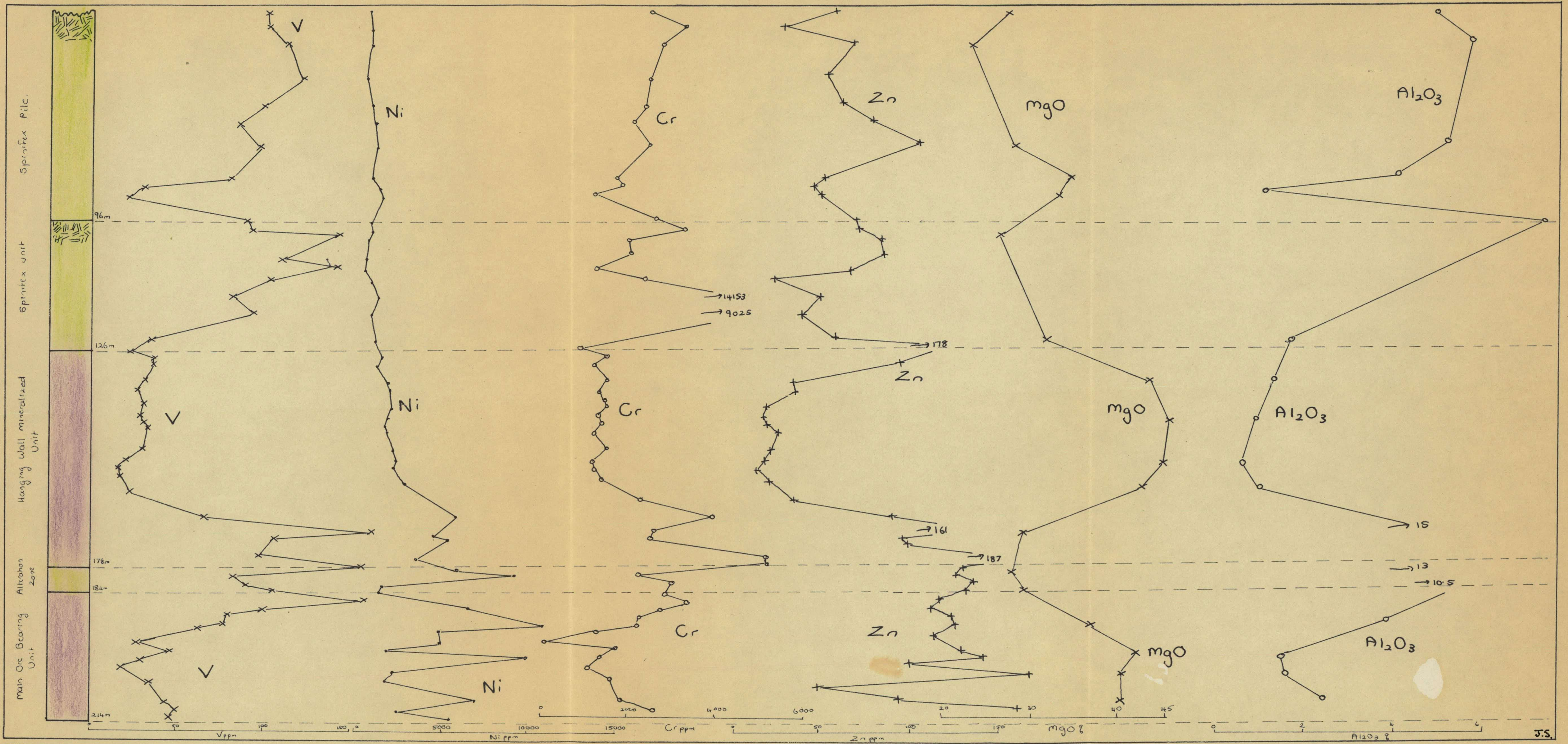

FIG. A Geochemical Section of WSD 23

WSD 104

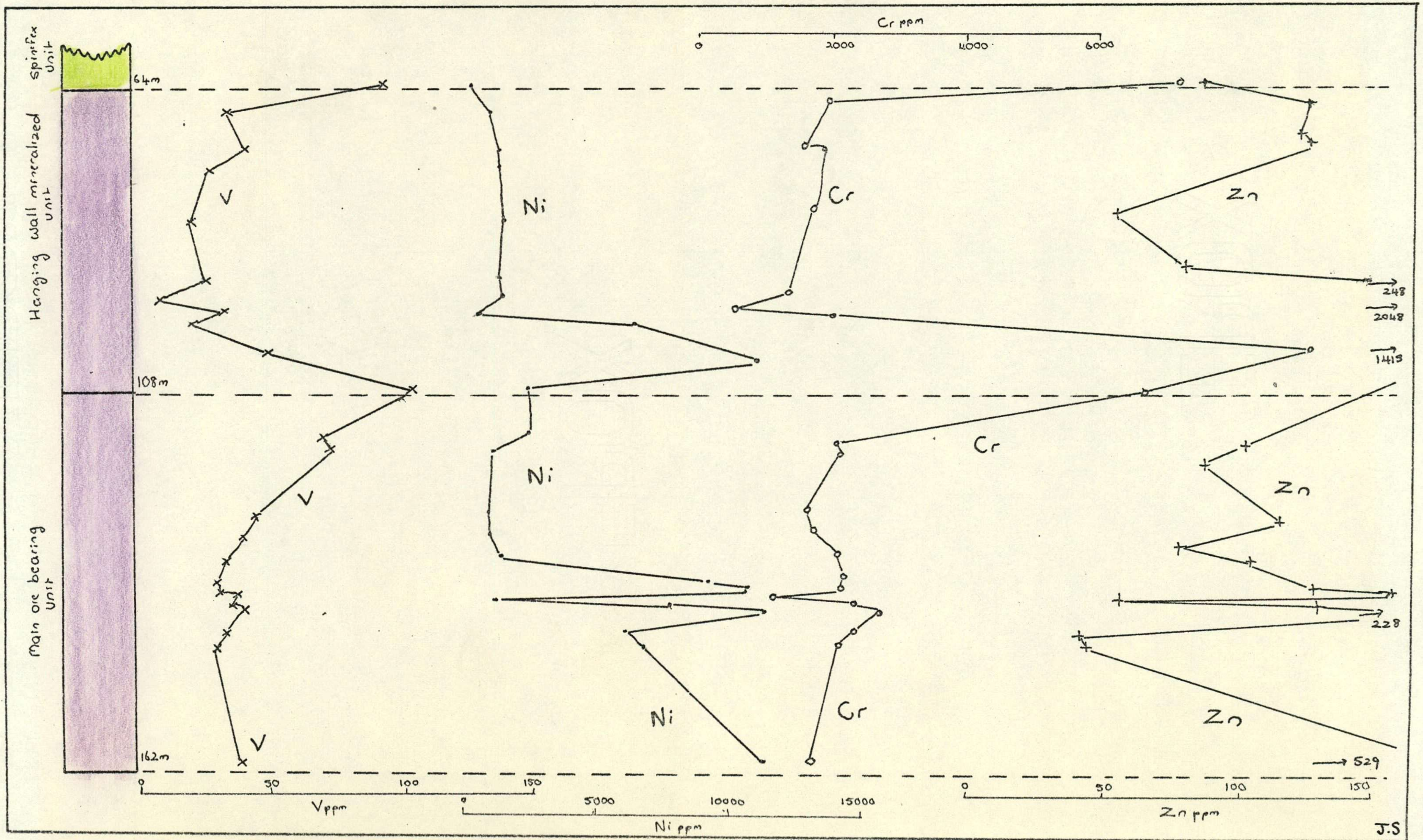

Fig. B. Geochemical Section of WSD 104

WSD 102.

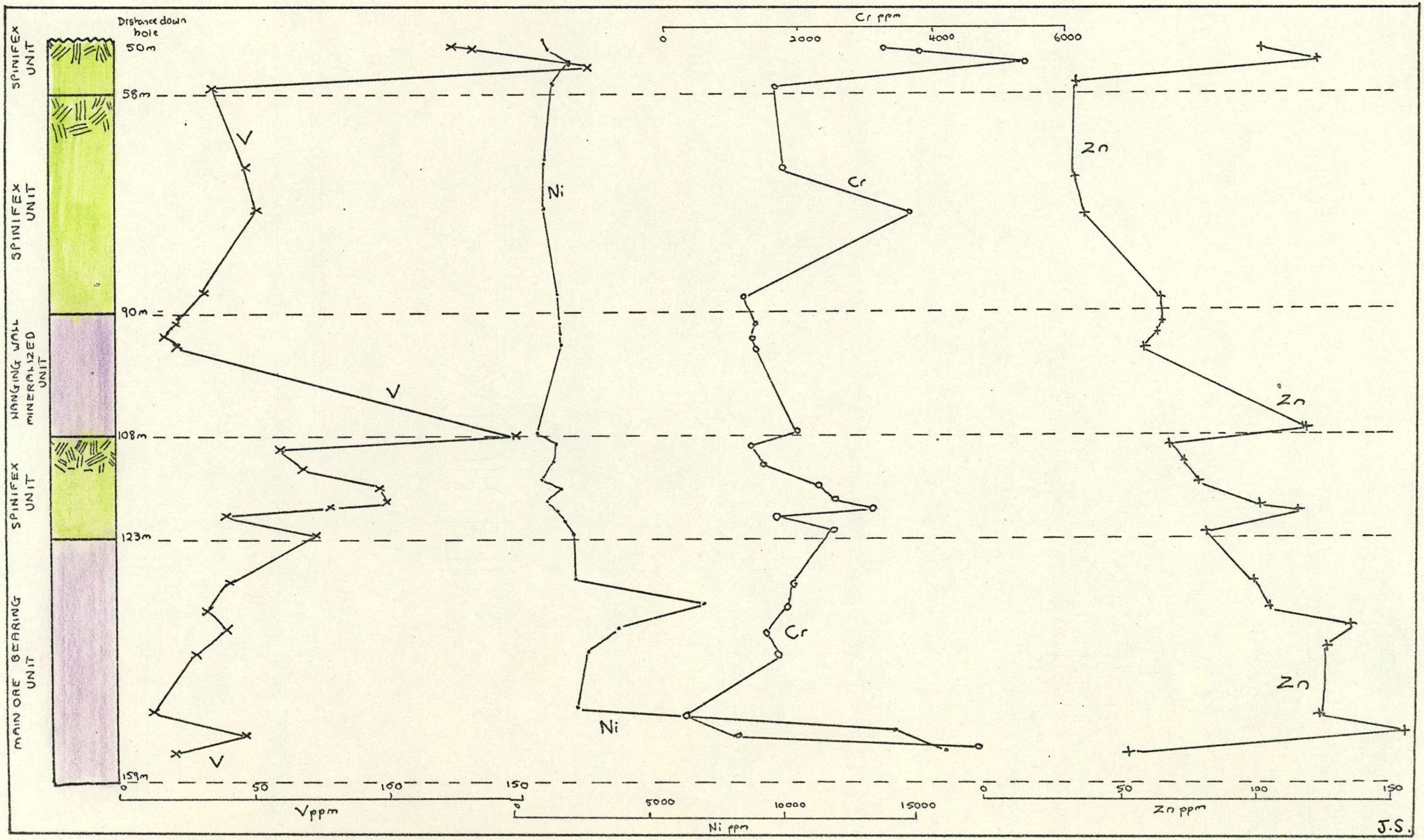

Fig. C. Geochemical Section of WSD 102

GS2

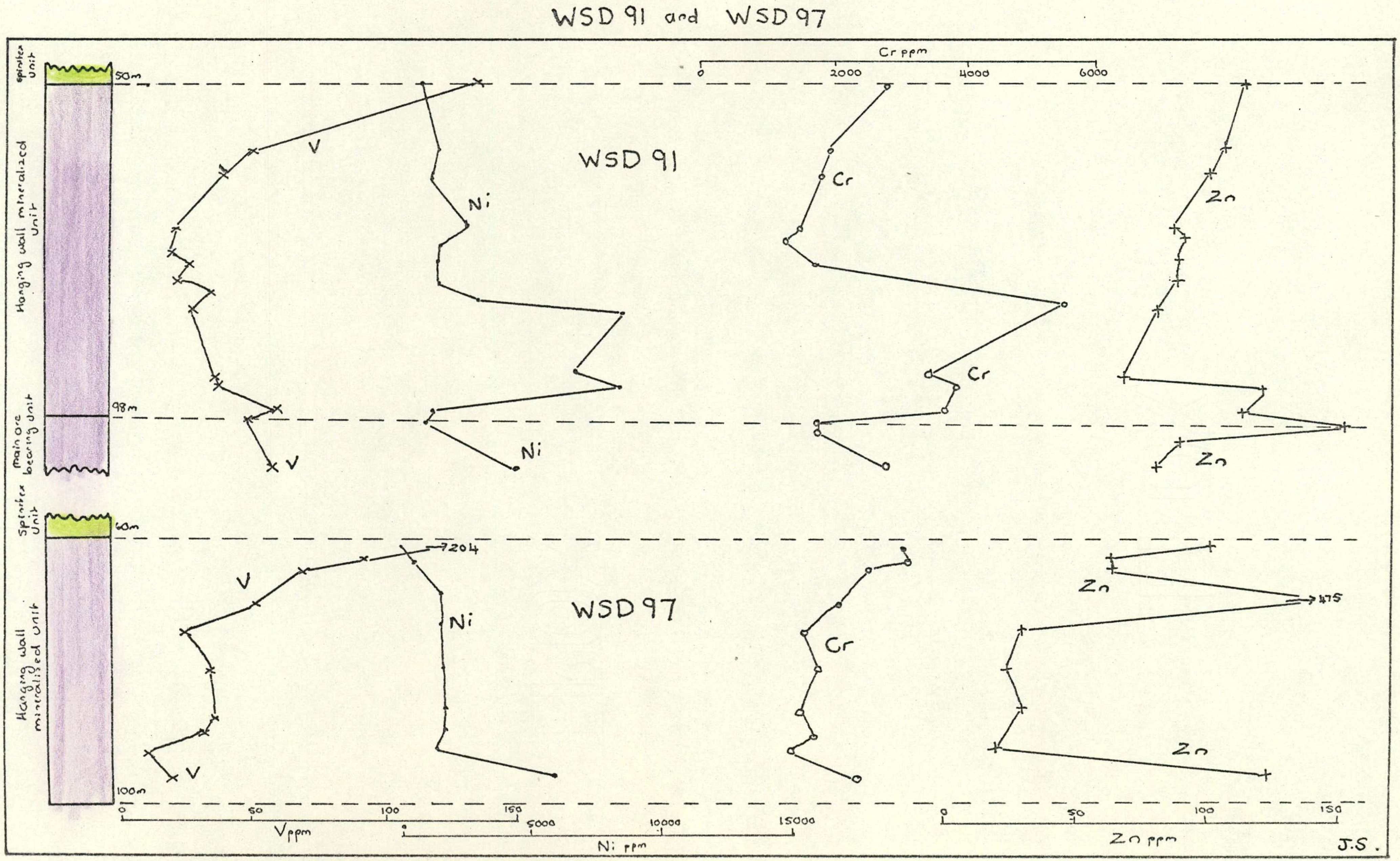

Fig. D Geochemical Sections of WSD 91, 97.

GS3

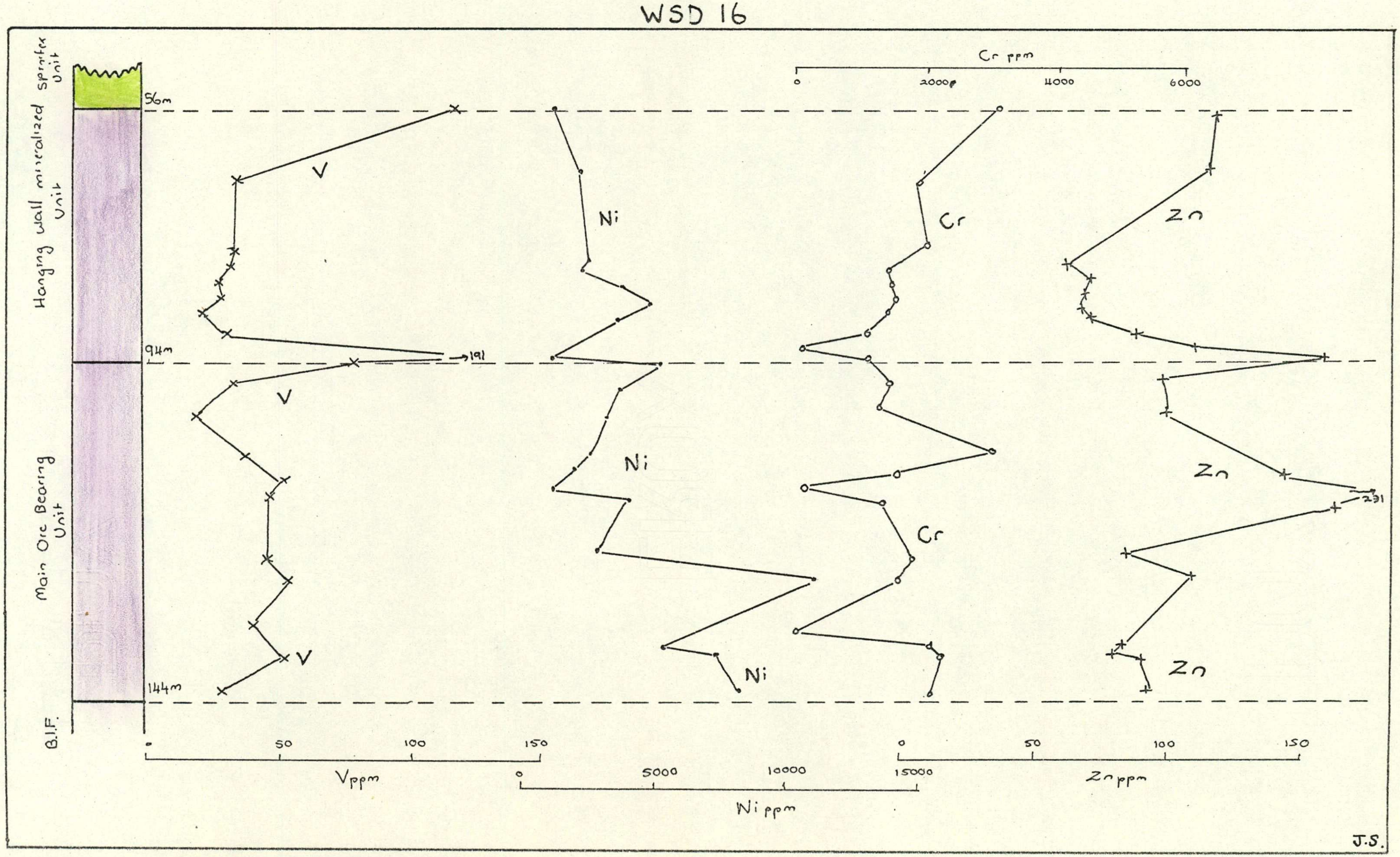

Fig. E. Geochemical Section of WSD 16

GS4

APPENDIX C

Whole Rock Analyses

WHOLE ROCK ANALYSES

One hundred and twenty whole rock analyses were made using the X-Ray fluorescence method as described by Norrish and Hutton (1968). The majority of analyses were concentrated on ultramafic rocks in order to exhibit trends in the major element chemistry across units and to compare barren units with mineralized ones. The results of these are tabulated in the next pages.

Other rock types (e.g. metabasalts, BIF and intrusions) were also analysed. Sodium was necessary on most of these, and was determined by flame photometry (analyst Lee Collins).

All fused buttons were made using material preheated to 1,000^{o}C for at least 6 hours after a previous heating to 110^{o}C overnight (H_2O^- values not determined). Weight loss was determined from the loss of a several gram sample in a silica crucible after the heating at 1,000^{o}C
This figure represents the sum of:

$$H_2O^+ \text{, S, C, and } Fe^{2+} \longrightarrow Fe^{3+}$$

Table C.1

Whole rock analyses

of WSD 93

	001	002	008	009	010	012	014	015	028	033	038	044
SiO_2	49.770	45.089	51.370	49.251	48.416	48.372	45.945	42.873	44.465	39.895	45.272	42.306
Al_2O_3	6.319	6.398	5.235	4.682	3.821	2.753	4.539	2.274	1.733	0.702	1.205	1.626
Fe_2O_3	11.761	14.760	5.389	5.424	7.054	7.422	6.002	8.043	11.042	8.780	7.668	9.669
MnO	0.226	0.255	0.047	0.060	0.047	0.043	0.133	0.152	0.061	0.141	0.076	0.122
MgO	23.568	24.159	37.678	41.111	39.529	40.444	42.069	43.615	42.343	49.068	45.161	46.052
CaO	8.718	7.364	0.046	0.177	0.054	0.059	0.995	1.102	0.159	1.213	0.378	0.084
K_2O	0.057	0.051	0.063	0.025	0.064	0.042	0.036	0.046	0.034	0.053	0.061	0.021
TiO_2	0.336	0.258	0.105	0.085	0.106	0.085	0.402	0.216	0.073	0.054	0.059	0.063
P_2O_5	0.057	0.054	0.029	0.005	0.029	0.017	0.021	0.009	0.009	0.011	0.070	0.009
TOTAL	100.810	98.388	99.962	100.819	99.120	99.238	100.141	99.329	99.919	99.918	99.890	99.951
Loss	4:66	5.12	9.49	11.08	10.30	11.00	14.02	16.12	13.16	20.62	15.27	16.04

TABLE C.1 WSD 93

	047	050	053	058	060	064	065	066	067	069	071	073
SiO_2	44.341	44.053	42.811	39.980	43.508	50.321	53.346	37.818	41.128	44.941	45.023	44.891
Al_2O_3	1.588	1.301	1.853	1.970	2.216	2.017	1.525	16.483	2.286	2.142	2.327	2.247
Fe_2O_3	10.303	11.418	11.371	15.326	12.174	10.498	11.961	9.774	15.150	9.957	8.006	8.955
MnO	0.075	0.084	0.060	0.112	0.097	0.134	0.062	0.162	0.155	0.049	0.042	0.045
MgO	43.043	41.987	41.929	41.284	40.496	36.498	30.723	34.896	38.110	42.471	43.032	41.977
CaO	0.206	0.262	0.032	0.298	0.056	0.542	0.597	0.029	1.239	0.160	0.066	0.185
K_2O	0.020	0.018	0.027	0.027	0.033	0.028	0.032	0.314	0.049	0.048	0.070	0.043
TiO_2	0.064	0.056	0.096	0.175	0.095	0.100	0.071	0.250	0.119	0.075	0.123	0.080
P_2O_5	0.007	0.005	0.016	0.013	0.013	0.009	0.003	0.014	0.019	0.009	0.011	0.016
TOTAL	99.648	99.184	98.194	99.187	98.688	100.147	98.319	99.74	98.255	99.851	98.700	98.438
Loss	12.61	11.51	11.74	12.80	12.50	9.43	7.02	11.12	11.78	11.41	12.04	11.52

	076	078	080	081	083	084	086	087	089	091	093	100
SiO_2	43.971	44.952	47.860	39.433	40.373	44.296	41.683	43.739	43.240	43.249	37.795	24.971
Al_2O_3	1.781	1.908	1.825	1.618	2.038	2.112	1.905	2.072	2.337	2.667	3.319	8.857
Fe_2O_3	11.353	10.48	9.805	19.001	12.763	10.180	13.645	11.548	12.317	9.599	17.306	41.471
MnO	0.147	0.164	0.142	0.184	0.119	0.048	0.073	0.046	0.110	0.147	0.133	0.120
MgO	39.254	41.223	39.859	37.275	42.621	41.468	39.611	41.472	40.795	43.211	38.291	19.531
CaO	0.957	0.984	0.030	0.659	0.059	0.073	0.153	0.053	0.026	0.273	0.067	4.836
K_2O	0.048	0.017	0.025	0.042	0.040	0.049	0.028	0.039	0.048	0.051	0.029	0.085
TiO_2	0.076	0.125	0.071	0.079	0.080	0.081	0.130	0.071	0.109	0.124	0.135	0.029
P_2O_5	0.015	0.007	0.012	0.018	0.011	0.011	0.026	0.023	0.014	0.015	0.024	0.026
TOTAL	97.601	99.860	99.629	98.309	98.103	98.319	97.254	99.062	98.994	99.316	97.098	99.866
Loss	11.93	12.03	10.52	14.14	15.86	11.87	11.93	11.96	11.88	15.25	16.33	20.13

SiO_2	
Al_2O_3	
Fe_2O_3	
MnO	
MgO	
CaO	
K_2O	
TiO_2	
P_2O_5	
TOTAL	
Loss	

TABLE C.1 WSD 93

Table C.2

Whole rock analyses

of WSD 100

TABLE C.2 WSD 100

	110	113	118	122	125	127	130	153	155	158	161
SiO_2	46.368	48.496	46.645	48.036	53.035	47.686	34.094	50.905	50.348	47.992	43.201
Al_2O_3	7.879	7.154	7.738	6.347	3.803	7.677	4.276	5.717	5.570	2.958	1.012
Fe_2O_3	12.961	11.521	13.469	11.384	8.201	11.332	5.914	9.067	9.485	7.447	7.828
MnO	-	-	-	-	-	-	-	-	-	-	-
MgO	29.788	28.630	28.874	25.807	24.942	27.759	29.697	25.389	26.817	42.476	44.904
CaO	1.084	3.860	2.335	7.402	9.959	3.851	23.999	9.085	8.680	0.149	1.987
K_2O	0.091	0.114	0.131	0.037	0.061	0.041	1.886	0.030	0.097	0.043	0.083
TiO_2	0.396	0.379	0.401	0.311	0.191	0.378	0.132	0.265	0.246	0.127	0.041
P_2O_5	0.037	0.024	0.041	0.032	0.042	0.056	0.042	0.033	0.328	0.139	0.043
TOTAL	98.583	100.168	99.634	99.357	100.235	98.780	100.040	100.491	101.570	101.331	99.099
Loss	7.81	7.26	7.56	6.00	5.86	4.32	28.82	5.01	5.49	11.47	7.00

	165	179	185	189	192	194	196	199	202	207	208
SiO_2	45.443	42.800	44.493	44.283	33.098	43.931	56.483	42.697	44.076	46.961	39.128
Al_2O_3	7.952	3.053	2.486	2.306	23.425	1.813	1.641	1.861	1.859	2.484	13.253
Fe_2O_3	11.488	7.644	8.937	8.786	8.724	7.735	7.316	6.477	7.051	7.575	7.930
MnO	-	-	-	-	-	-	-	-	-	-	-
MgO	29.657	40.853	40.866	41.380	34.455	44.207	34.583	42.884	42.997	42.006	34.983
CaO	4.645	3.866	3.294	2.947	0.076	1.483	0.023	4.662	2.760	0.094	2.111
K_2O	0.012	0.039	0.006	0.007	0.010	0.007	0.026	0.004	0.005	0.008	0.184
TiO_2	0.430	0.134	0.107	0.103	0.185	0.077	0.075	0.079	0.08	0.279	0.100
P_2O_5	0.044	0.041	0.022	0.010	0.050	0.015	0.014	0.018	0.007	0.066	0.467
TOTAL	99.670	98.430	100.211	99.821	100.025	99.268	100.162	98.681	98.836	99.473	98.236
Loss	7.03	1.83	13.83	13.77	11.98	15.17	6.97	15.74	14.11	11.46	10.64

TABLE C.2 WSD 100

	210	213	216	217	222	224	226	227	233	236	241
SiO_2	43.002	48.559	48.559	48.559	39.288	46.038	50.699	46.414	47.108	44.823	40.713
Al_2O_3	3.700	3.696	4.183	6.186	3.922	4.291	3.429	4.820	2.732	2.894	1.857
Fe_2O_3	10.011	13.054	9.759	10.419	9.755	13.11	9.571	11.474	7.833	8.017	13.820
MnO	–	–	–	–	–	–	–	–	–	–	–
MgO	40.669	38.029	29.612	27.496	30.705	34.743	30.787	32.216	43.088	42.394	39.799
CaO	0.031	2.138	6.561	6.743	5.867	1.245	2.514	4.451	0.166	0.632	1.545
K_2O	0.010	0.017	0.050	0.008	0.014	0.010	0.011	0.009	0.008	0.000	0.000
TiO_2	0.207	0.195	0.214	0.291	0.245	0.242	0.141	0.212	0.117	0.174	0.088
P_2O_5	0.019	0.022	0.031	0.036	0.022	0.016	0.013	0.263	0.109	0.027	0.258
TOTAL	99.448	100.183	98.969	99.738	99.817	99.697	97.165	99.860	101.153	99.762	97.880
Loss	11.5	11.35	8.16	4.71	6.99	9.00	6.68	7.83	11.72	11.56	11.21

	246	250	251	252	256
SiO_2	45.164	36.515	30.657	55.748	34.783
Al_2O_3	2.155	1.508	19.868	1.203	1.282
Fe_2O_3	11.325	21.775	19.485	11.814	39.236
MnO	–	–	–	–	–
MgO	40.747	34.931	29.283	26.218	17.412
CaO	0.029	1.689	0.269	3.857	4.062
K_2O	0.001	0.000	0.006	0.006	0.005
TiO_2	0.094	0.073	1.834	0.049	0.059
P_2O_5	0.156	0.020	0.182	0.016	0.017
TOTAL	99.669	96.511	101.582	98.913	96.857
Loss	11.2	10.88	3.73	4.35	8.17

TABLE C.2 (Contd.) WSD 100

Table C.3

Whole rock analyses

of WSD 23

	347	354	367	371	375	380	396	403	417	423	428
SiO_2	50.617	49.768	45.680	41.341	40.083	43.312	45.598	45.627	42.578	42.889	36.740
Al_2O_3	5.373	6.119	5.530	4.396	1.314	8.505	1.997	1.845	0.801	1.169	14.998
Fe_2O_3	9.953	10.282	10.435	8.889	6.937	15.242	6.832	6.319	9.179	11.129	12.484
MnO	0.149	0.211	0.205	0.215	0.334	0.187	0.327	0.104	0.105	0.088	0.247
MgO	28.114	24.328	29.278	35.509	33.624	27.790	32.536	43.943	45.577	42.497	29.143
CaO	4.033	8.301	5.698	7.768	16.105	3.308	9.942	0.456	0.553	0.148	2.226
K_2O	0.012	0.041	0.032	0.072	0.023	0.013	0.008	0.004	0.111	0.032	0.100
TiO_2	0.265	0.281	0.265	0.172	0.054	0.463	0.097	0.075	0.043	0.051	0.385
P_2O_5	0.017	0.036	0.033	0.051	0.031	0.039	0.026	0.016	0.038	0.009	0.063
TOTAL	98.384	99.156	96.951	98.198	98.171	98.671	97.036	98.286	98.882	97.924	96.139
Loss	6.14	5.37	10.58	16.99	23.81	6.72	16.23	12.50	14.31	12.41	9.54

	433	440	443	447	454	457	460
SiO_2	34.170	42.823	43.773	36.090	40.529	44.733	40.925
Al_2O_3	12.935	4.058	3.843	16.494	1.731	1.857	2.530
Fe_2O_3	16.453	12.883	10.019	7.541	13.105	10.187	8.790
MnO	0.235	0.213	0.207	0.122	0.123	0.154	0.164
MgO	29.694	36.890	38.793	36.808	40.419	42.364	41.693
CaO	2.513	0.725	0.249	0.313	1.203	0.346	3.776
K_2O	0.144	0.013	0.023	0.065	0.018	0.000	0.024
TiO_2	0.553	0.215	0.178	0.269	0.082	0.098	0.158
P_2O_5	0.037	0.013	0.014	0.039	0.013	0.015	0.001
TOTAL	96.500	97.620	96.854	97.619	97.101	99.597	97.894
Loss	9.33	10.98	11.31	11.88	11.52	11.14	13.22

TABLE C.3 - WSD 23

APPENDIX D

Trace Element Analyses

TRACE ELEMENT ANALYSES

Samples were analysed by the Phillips PW/1510 X-Ray fluorescence spectrometer, on pressed buttons, made from the crushed portions done in the tungsten steel vessel on the Siebtechnik Mill. Shaking on the mill was ceased after 4 minutes.

Elements analysed were Ni, Zn, V and Cr (Cr was done on the Siemens X-Ray spectrometer) under the following conditions:

	Ni	Zn	V	Cr
Tube	Au	Au	W	Mo
KV/ma	60/40	60/40	60/40	60/40
LIF crystal	220	220	220	200
Collimator	Coarse	Coarse	Coarse	Coarse
Counter	Scintill-ation	Scintill-ation	Flow Prop	Scintill-ation
Air	Air	Air	Vacuum	Vacuum
Counting Time	100 sec	100 sec	100 sec	100 sec

TABLE D.1 Conditions for Trace Element Analysis

Sulphur was analysed by ignition of a known quantity of sample, and titration of SO_2 released, against a standard solution. This was done on the Leco automatic sulphur determination equipment.

WSD 93

Sample No	Distance down hole (m)	Geology	Ni	Cr	Zn (p·p·m)	V	S
001	56	Spinifex Unit	1101	1515	110	120	260
002	58		1315	1.30%	164	151	90
004	60	Hanging Wall Mineralized Unit	1237	6443	168	63	40
005	61		1200	4857	159	60	
006	64		1208	1112	150	54	
007	65		1238	897	121	60	
008	65.5		1152	1499	114	61	35
009	66		1404	1579	79	59	
010	67		1903	1745	70	63	1140
011	68		1555	1929	72	48	
015	72		1869	1877	100	50	1880
016	74		1437	2211	67	45	
017	74.5		1220	1649	70	32	
025	83		2075	1300	80	37	2320
026	85		1873	1429	75	41	
027	85.5		2036	1596	76	33	
028	86		2060	1763	105	40	980
031	88		1884	849	89	43	
033	90		1209	261	79	18	4280
037	93		1200	1274	78	21	
038	94		1884	1408	83	22	1280
039	95		2390	1509	103	24	
044	99		2275	1581	46	14	
047	100		2275	3742	29	32	1960
050	103		6354	3807	58	31	
051	104		4442	4197	40	40	
053	105		6830	4652	40	50	5640
055	107		2048	6351	35	52	
056	108		2034	4422	48	42	
057	110		2313	4547	32	33	1320
058	110.5		3162	5066	34	67	
059	111		2415	4013	38	34	
060	112		2250	5717	87	48	1480
062	115		2680	3624	118	36	
063	116		3601	18	52	18	
064	118		2018	4156	106	38	1360
065	119		2841	2961	87	35	4240
066	120		860	2027	167	44	60
067	120.1	Main ore bearing unit	2411	5120	78	61	4280
068	121		2108	2815	51	48	
069	123		1799	2262	56	38	1320
070	124		1744	2446	37	29	
071	126		4880	2103	41	46	
073	128		3307	2141	135	30	
074	128.5		4651	1353	38	33	4360
075	130		2356	2042	87	60	
076	132		6572	2213	97	33	1.2%

WSD 93 (Continued)

Sample No.	Distance (m)	Geology	Ni	Cr	Zn (p.p.m)	V	S
078	136	Main ore bearing unit	1650	1772	93	34	2440
080	138		1639	1442	104	31	2240
081	139		5736	2208	93	43	1.44%
084	144		5141	1976	34	40	1.36%
085	145		9209	2088	31	47	
086	146		8851	2103	38	65	
087	147		7080	1704	35	38	1.76%
088	150		5148	1628	39	41	
089	151		6838	1752	64	52	
090	152		9953	2023	83	54	2.52%
091(1)	152.1		3256	1589	83	39	
091(4)	153		8262	1553	89	33	
092	154		1.32%	1146	86	50	4.08%
093	156		1.40%	2531	134	44	
094	157		2.14%	3671	131	48	14.48%
097(1)	161		2.43%	4826	532	57	18.00%
097(2)	162		1.19%	2163	693	54	14.00%
100	164		1.56%	2959	244	41	12.92%

WSD 100

Sample No.	Distance	Geology	Ni	Cr	Zn (p.p.m)	V	S
110	31		1740	3555	106	124	40
111	32	Spinifex	1008	2522	70	89	
113	34	Unit	1317	3856	104	127	
115	37		1422	3852	105	142	70
118	44		1532	4039	111	137	
120	47		1170	3232	66	97	100
121	48	Spinifex	1511	3661	108	127	
122	49	Unit	1341	3316	99	127	60
124	51		983	3379	101	134	
125	52		942	2489	77	91	70
126	53		1088	3365	92	116	70
129	55		873	2105	87	64	
130	58		1325	1220	97	50	70
153	86	Spinifex	1086	2910	93	120	540
155	88	Unit	1155	3034	137	107	2920
157	91		1708	3120	88	45	
158	93		1625	2354	72	19	1080
160	96		1847	1530	84	17	
161	97		1774	1169	64	60	3200
163	99		1201	2191	53	89	
164	99.5		1145	2905	66	137	3200
165	101		883	2639	71	137	2320
175	111	Spinifex	209	1574	172	163	60
176	112	Unit	382	3098	102	160	70
178	115		78	505	72	97	
179	116		79	757	90	161	
182	120		1298	5829	62	63	2680
183	121		1277	2371	46	75	
185	122		1602	1776	60	39	3880
186	124		1671	1923	61	41	
187	125		1655	1880	58	42	
189	127		1732	2102	64	45	3280
190	128	Hanging	1592	2021	60	34	
191	129	Wall	1663	2121	50	25	3720
192	130	Mineralized	249	99	121	28	140
194	132	Unit	1903	1541	57	30	2360
195	133		1743	1623	98	26	
196	134		1585	1601	82	27	1120
197	135		1856	1590	59	26	
198	137		1602	1598	53	26	
199	138		1566	1795	53	28	1080
201	140		1952	1844	51	27	
202	143		1701	1580	56	34	920
203	145		1903	1413	60	24	
205	146		2102	1386	113	17	
206	147		4843	1632	71	17	7640
207	148		2892	1295	115	34	
208	149		2599	2280	116	44	3880
209	149.5		6928	2410	95	20	
210	150		2224	4322	115	59	3080

WSD 100 (Continued)

Sample No.	Distance	Geology	Ni	Cr	Zn (p.p.m)	V	S
211	151		2499	2225	106	65	
213	152		3124	4187	113	59	7080
214	153		2197	3780	98	54	4520
215	153.5		1944	4569	108	70	3480
216	156		1319	3176	62	76	
217	158		1125	3334	60	103	2960
219	160	Barren	1629	3411	86	160	
220	161	Spinifex	1178	3245	63	78	80
221	162	Unit	1463	3573	69	78	
222	163		1731	2114	99	55	1.15%
224	164		1625	2664	118	68	
225	165		1704	1981	114	56	8080
226	166		1320	2638	106	55	1.44%
227	167		2221	2276	97	64	
229	169		1745	2017	99	73	4600
233	172		2235	1831	128	40	
234	174		7516	1935	103	46	1.40%
236	173		3531	1879	117	48	
237	176		1961	1771	102	41	3000
239	179	Main	6869	1699	74	38	
240	180	Ore	6713	1963	75	35	1.44%
241	181	Unit	8110	1769	72	36	
242	182		9236	1801	93	32	3.04%
245	186		5133	2100	100	49	1.60%
247	187		1.30%	2394	51	43	
248	188		1.47%	2071	40	37	4.40%
250	189		1.00%	1224	100	50	2.40%
252	193		3496	1100	233	22	2.34%
253	195		1.75%	2323	180	61	
256	197		1.82%	1701	244	55	11.52%

WSD 23

Sample No.	Distance (m)	Geology	Ni	Cr (p.p.m)	Zn	V
344	46		996	2771	70	92
347	48		1219	2772	68	99
351	53		1187	3013	31	99
354	56		1338	2994	74	108
358	64		969	2728	59	117
361	69	Spinifex	1353	2686	67	96
364	72	Unit	1589	2331	84	79
367	77		1579	2753	112	91
371	87		1371	2070	54	71
372	88		1578	2150	48	29
375	92		1705	1497	52	19
377	97		1126	2913	74	85
378	98		1165	3662	74	89
380	99		903	2284	89	141
383	104		881	2351	88	111
385	106		601	1428	70	142
389	112	Spinifex	1025	2645	26	99
390	114	Unit	1464	1.415%	53	79
396	124		1221	2675	60	34
397	125		1507	1046	178	18
399	129		1663	1758	74	34
400	130		1385	1444	96	33
403	136		2066	1715	37	29
404	137		2121	1501	38	26
406	141		2265	1736	21	30
408	144	Hanging	1945	1516	20	28
410	147	Wall	1838	1643	20	32
411	149	Mineralized	1917	1425	28	33
413	151	Unit	2055	1717	18	30
416	157		2329	1436	16	18
417	158		2150	1421	12	15
421	165		2894	1698	23	16
423	170		6287	2557	36	22
426	172		4383	4267	93	66
428	173		5371	4260	161	162
429	174		3236	2874	97	105
431	178		5975	2729	98	96
433	180		6637	5501	177	158
434	182	Alteration	9512	2435	132	79
435	183	Zone	1584	3366	127	90
436	184		1319	3020	140	114
437	186		1.60%	3590	133	157
438	187		6663	3083	118	110
439	188		1.54%	2581	112	82
440	191		1.19%	2488	126	78
443	194	Main	4868	2387	128	62
446	197	Ore	4751	1514	112	24
447	198	Unit	1338	247	136	48
448	200		1.01%	1906	144	33
450	201		2330	1648	97	28
451	203		1494	1252	231	16

WSD 23 (Continued)

Sample No.	Distance (m)	Geology	Ni	Cr (p.p.m)	Zn	V
454	206	Main Ore Unit	7037	1822	47	34
457	211		2383	1849	94	41
459	214		5290	2026	164	48
460	216		1589	1829	170	45

WSD 104

Sample No.	Distance (m)	Geology	Ni	Cr	Zn	V
				(p.p.m)		
651	162	Main Ore Unit	1.19%	1311	529	40
652	145		7449	1862	48	32
653	143		6487	1975	44	34
654	141		1.21%	2393	228	42
655	139.6		8561	2069	139	36
656(2)	139.5		920	23	58	44
565(1)	139.2		1.23%	1790	165	32
657	136		1.02%	1844	132	33
658	135		2000	1792	120	33
659	133		2093	1337	113	34
660	130		1715	1312	80	40
661	126		1641	1868	122	45
662	117		1423	1768	91	75
663	115		3078	2021	109	71
664	107		2953	6325	162	104
665A	104	Hanging Wall Mineralised Zone	1.27%	8909	1415	53
665	98		7008	4261	2032	18
666	97		810	366	248	48
667	967		1856	1132	654	12
668	92		1776	1127	88	28
670	83		2075	1449	61	23
671	73		1931	1712	134	43
672	75		1852	1287	132	30
674	67		1469	1665	134	36
675	63	Spinifex Unit	753	6924	94	96

WSD 102

Sample No.	Distance (m)	Geology	Ni	Cr (p.p.m)	Zn	V
613	51	Spinifex Unit	848	3384	114	125
614	52		1019	3915	114	140
615	54		2205	5366	137	178
616	57		1377	1648	47	33
617	69		1291	1866	46	47
618	76	Spinifex Unit	1170	3906	48	51
619	88		1604	1273	50	22
620	92	Hanging Wall Mineralized Unit	1599	1415	79	16
621	94		1780	1407	78	23
622	95		2080	1389	71	22
624	108	Spinifex Unit	646	2110	137	161
625	110		1485	1381	79	69
626	113		1352	1665	87	69
627	116		750	2465	92	96
628	118		2209	2660	114	76
629	119		1171	3239	130	39
630	120		1560	1712	91	76
631	123	Main Ore	1912	2594	112	41
632	130		1838	1997	112	32
633	134		7027	1842	117	41
634	137		3867	1587	148	40
635	139		2851	1626	134	27
636	149		2047	1063	133	11
637	152		1.44%	60	163	49
639	155		1.64%	4705	61	22

WSD 91

Sample No.	Distance (m)	Geology	Ni	Cr (p.p.m)	Zn	V
711	48	Spinifex Unit	1566	2786	120	135
712	61	Hanging Wall Mineralized Unit	1936	1904	112	53
713	64		1861	1758	105	44
714	72		2915	1464	93	23
715	75		2067	1229	97	23
716	77		2085	1779	95	29
717	79		2086	1995	94	23
718	81		3646	5620	86	41
719	84		9137	3389	74	28
720	94		7203	3909	127	42
721	95		9375	3852	118	42
722	99		2045	3674	157	66
723	100	Main Ore Unit	1710	1639	96	53
724	108		4839	2733	84	61

WSD 97

Sample No.	Distance (m)	Geology	Ni	Cr (p.p.m)	Zn	V
676	62	Spinifex Unit	670	3062	103	204
677	66	Hanging Wall Mineralized Unit	1061	3119	64	87
678	67		1983	2414	65	71
679	70		1909	1961	475	53
680	74		2199	1462	32	26
681	80		2061	1776	35	34
682	85		2091	1435	30	36
683	89		2156	1664	22	32
683B	92		1941	1204	18	13
684	96		6253	2213	124	20
686	99		4633	2456	85	22
687	100		5784	2475	1099	23

WSD 16

Sample No.	Distance (m)	Geology	Ni	Cr (p.p.m)	Zn	V
686	143	Main Ore Unit	7841	2181	94	31
687	137		7112	2000	92	53
688	136		4729	2102	81	49
690	132		4149	2020	86	40
691	127		11040	1596	116	58
692	123		2381	1852	86	48
694	114		3753	1339	168	50
695	114	Chlorite Schist	365	50	231	57
696	108		2033	3307	149	41
697	102		2657	1339	105	19
698	97		3052	1280	101	35
699	94		4471	1218	164	82
700	93.9	Chlorite schist	138	250	115	191
701	92	Hanging Wall Mineralized Unit	3394	1534	90	35
702	90		3237	1704	90	32
703	87		4274	1974	74	22
704	86		2980	1670	71	32
705	84		2989	1691	74	29
706	82		1562	1835	76	33
707	80		2080	1831	65	35
708	72		1841	1522	80	30
709	67		1426	2116	122	35
710	56	Spinifex Units	1077	3319	125	119